

The Dual Dopamine-Glutamate Phenotype of Growing Mesencephalic Neurons Regresses in Mature Rat Brain

NOÉMIE BÉRUBÉ-CARRIÈRE,¹ MUSTAPHA RIAD,¹ GRÉGORY DAL BO,² DANIEL LÉVESQUE,³
LOUIS-ÉRIC TRUDEAU,^{2,3} AND LAURENT DESCARRIES^{1,4,5*}

¹Department of Pathology and Cell Biology, Faculty of Medicine, Université de Montréal, Montréal, Québec, Canada H3C 3J7

²Department of Pharmacology, Faculty of Medicine, Université de Montréal, Montréal, Québec, Canada H3C 3J7

³Faculty of Pharmacy, Université de Montréal, Montréal, Québec, Canada H3C 3J7

⁴Groupe de Recherche sur le Système Nerveux Central, Université de Montréal, Montréal, Québec, Canada H3C 3J7

⁵Department of Physiology, Faculty of Medicine, Université de Montréal, Montréal, Québec, Canada H3C 3J7

ABSTRACT

Coexpression of tyrosine hydroxylase (TH) and vesicular glutamate transporter 2 (VGLUT2) mRNAs in the ventral tegmental area (VTA) and colocalization of these proteins in axon terminals of the nucleus accumbens (nAcb) have recently been demonstrated in immature (15-day-old) rat. After neonatal 6-hydroxydopamine (6-OHDA) lesion, the proportion of VTA neurons expressing both mRNAs and of nAcb terminals displaying the two proteins was enhanced. To determine the fate of this dual phenotype in adults, double in situ hybridization and dual immunolabeling for TH and VGLUT2 were performed in 90-day-old rats subjected or not to the neonatal 6-OHDA lesion. Very few neurons expressed both mRNAs in the VTA and substantia nigra (SN) of P90 rats, even after neonatal 6-OHDA. Dually immunolabeled

terminals were no longer found in the nAcb of normal P90 rats and were exceedingly rare in the nAcb of 6-OHDA-lesioned rats, although they had represented 28% and 37% of all TH terminals at P15. Similarly, 17% of all TH terminals in normal neostriatum and 46% in the dopamine neoinnervation of SN in 6-OHDA-lesioned rats were also immunoreactive for VGLUT2 at P15, but none at P90. In these three regions, all dually labeled terminals made synapse, in contradistinction to those immunolabeled for only TH or VGLUT2 at P15. These results suggest a regression of the VGLUT2 phenotype of dopamine neurons with age, following normal development, lesion, or sprouting after injury, and a role for glutamate in the establishment of synapses by these neurons. *J. Comp. Neurol.* 517:873–891, 2009.

© 2009 Wiley-Liss, Inc.

Indexing terms: neoinnervation; neostriatum; nucleus accumbens; substantia nigra; tyrosine hydroxylase; ventral tegmental area; vesicular glutamate transporter 2

Since the first demonstration that an inorganic phosphate carrier was able to concentrate glutamate in synaptic vesicles (Ni et al., 1994), three proteins capable of playing that role have been identified in mammalian central nervous system and were therefore given the names of *vesicular glutamate transporters 1, 2, and 3* (VGLUT1–3; for review see Freneau et al., 2004; Liguz-Lecznar and Skangiel-Kramska, 2007; Trudeau, 2004). In adult rat brain, the expression patterns of VGLUT1 and VGLUT2 are largely complementary, VGLUT1 mRNA being widely found in pyramidal neurons of the neocortex and hippocampus and in cerebellar cortex, whereas VGLUT2 mRNA predominates in diencephalic and other subcortical nuclei, deep cerebellar nuclei, and the brainstem (Bai et al., 2001; Freneau et al., 2001; Herzog et al., 2001; Ni et al., 1995). A third vesicular glutamate transporter has also been cloned, which shows a more restricted expression by neurons not classically considered to be glutamatergic, notably serotonin neurons of the midbrain raphe and cholinergic neurons of the striatum and forebrain (Boulland et al., 2004; Gras et al., 2002, 2008; Harkany et al., 2003; Schafer et al., 2002; Taka-

mori et al., 2002). There is also considerable in situ hybridization and immunocytochemical evidence for a colocalization of VGLUT2 in catecholaminergic neurons, notably in noradrenaline neurons of the A2 group and adrenaline neurons of the C1,

Additional Supporting Information may be found in the online version of this article.

Grant sponsor: Canadian Institutes of Health Research; Grant number: MOP-3544 (to L.D.); Grant number: MOP-49951 (to L.-É.T.); Grant sponsor: National Alliance for Research on Schizophrenia and Depression (to L.-É.T.); Grant sponsor: Fonds de la Recherche en Santé Québec (to the Groupe de Recherche sur le Système Nerveux Central).

*Correspondence to: Laurent Descarries, MD, Department of Pathology and Cell Biology, Faculty of Medicine, Université de Montréal, C.P. 6128, Succursale Centre-Ville, Montreal, QC, Canada H3C 3J7.
E-mail: laurent.descarries@umontreal.ca

Received 25 February 2009; Revised 29 April 2009; Accepted 3 August 2009

DOI 10.1002/cne.22194

Published online August 10, 2009 in Wiley InterScience (www.interscience.wiley.com).

C2, and C3 groups of the medulla (Stornetta et al., 2002) and dopamine (DA) neurons of the mesencephalic groups A9 and A10 (Kawano et al., 2006; Yamaguchi et al., 2007).

Early evidence for the release of glutamate by mesencephalic DA neurons was obtained *in vitro*, in microcultures of isolated VTA neurons (Bourque and Trudeau, 2000; Sulzer et al., 1998) and cocultures of VTA DA neurons with GABAergic medium spiny neurons of the nucleus accumbens (nAcb; Joyce and Rayport, 2000). In a subsequent study in primary cultures of postnatal rat mesencephalic neurons, as many as 80% of isolated neurons immunopositive for tyrosine hydroxylase (TH), the biosynthetic enzyme of DA, were shown to be VGLUT2 immunopositive (Dal Bo et al., 2004). Different percentages were more recently reported in adult rat, in which 19% of TH-immunopositive neurons of the VTA were shown to express VGLUT2 mRNA (Kawano et al., 2006) and 0.1% of neurons to express both TH and VGLUT2 mRNA by double *in situ* hybridization (Yamaguchi et al., 2007). The discrepancy between the latter proportions probably reflected differences in experimental approach, but the large difference between *in vitro* and *in vivo* data was suggestive of a regulation of VGLUT2 expression in DA neurons during development and/or in response to injury.

In a recent study in late embryonic and postnatal rat, evidence was indeed obtained suggesting that the dual TH/VGLUT2 phenotype of mesencephalic DA neurons innervating the nAcb of rat was repressed at late embryonic stages and could be reactivated after neonatal 6-hydroxydopamine (6-OHDA) lesioning of these neurons (Dal Bo et al., 2008). In tissue sections of embryonic mesencephalon processed for dual *in situ* hybridization, there was a striking overlap between the labeling for TH and that for VGLUT2 mRNA at embryonic stages E14–E16, which was no longer found at stages E18–E21 or postnatally. Moreover, whereas only 1.8% of VTA neurons exhibiting TH mRNA signal were also labeled for VGLUT2 mRNA in normal 15-day-old rats (P15), this proportion increased to 26% of the surviving DA neurons in VTA after neonatal lesioning by cerebroventricular injection of 6-OHDA at P4. Finally, electron microscopic examination of the nAcb after dual immunolabeling for TH and VGLUT2 demonstrated the presence of VGLUT2 protein in 28% of TH axon terminals in normal P15 rats and in an even greater proportion (37%) of residual TH terminals in P15 rats 6-OHDA-lesioned at P4.

The general goal of the present study was to determine the fate of this dual dopamine/glutamate (TH/VGLUT2) phenotype with maturation of the brain. In particular, an answer was sought to the following questions. What is the proportion of DA neurons in normal adult rat VTA that coexpresses TH and VGLUT2 mRNA, and what is the frequency of colocalization of the two proteins in their DA axon terminals in nAcb? Does the reactivation of this double phenotype observed at P15 in rats neonatally lesioned with 6-OHDA persist in the adult? Are there TH-immunoreactive axon terminals colocalizing VGLUT2 in immature or mature rat neostriatum (NStr)? Does the aberrant DA neoinnervation that pervades the remnants of SN after a neonatal 6-OHDA lesion (Fernandes Xavier et al., 1994) display the dual TH/VGLUT2 phenotype? Are there morphological correlates, particularly in terms of synaptic features, of the existence of VGLUT2 in DA axon under these various conditions?

To answer these questions, double *in situ* hybridization for TH and VGLUT2 mRNA and dual immunolabeling of the two proteins at the electron microscopic level were used in adult (P90) as well as immature (P15) rats subjected or not to the neonatal cerebroventricular administration of 6-OHDA at P4. As in our prior studies (Dal Bo et al., 2008; Descarries et al., 2008), we focused on the nAcb, in which axon terminals from surviving DA neurons of the VTA are still found after the neonatal 6-OHDA lesion. We also examined DA terminals in the NStr of normal rats as well as the DA neoinnervation of the SN after neonatal 6-OHDA lesion. In all instances, quantitative data were obtained on the number of terminals singly (TH and VGLUT2) and dually (TH/VGLUT2) labeled in an equivalent area of thin section examined in each rat, as well as data on their intrinsic and synaptic features. Some of the results obtained in immature rat have already been published (Dal Bo et al., 2008; Descarries et al., 2008), but are included in the Tables to facilitate comparison with the adult.

MATERIALS AND METHODS

Animals

All procedures involving animals and their care were conducted in strict accordance with the *Guide to the care and use of experimental animals* (Ed. 2) of the Canadian Council on Animal Care. The experimental protocols were approved by the Comité de Déontologie pour l'Expérimentation sur des Animaux (CDEA) of the Université de Montréal. Sprague-Dawley male rats and pregnant dams were purchased from Charles River (St. Constant, Québec, Canada). Housing was at a constant temperature (21°C) and humidity (60%), under a fixed 12-hour light/dark cycle and with free access to food and water.

6-OHDA lesions

Neonatal 6-OHDA lesions were produced as previously described (Stachowiak et al., 1984; Jackson et al., 1988; Fernandes Xavier et al., 1994). In brief, 4-day-old pups (P4) received a subcutaneous injection of desipramine (25 mg/kg s.c.; Sigma, St. Louis, MO) 45 minutes before toxin injection to protect noradrenergic neurons. 6-OHDA hydrochloride (10 mg/ml; Sigma) was dissolved in artificial CSF containing 0.2% ascorbic acid to prevent oxidation. Pups were anesthetized on ice, immobilized on a cold body mould, and administered 5 μ l 6-OHDA solution (i.e., 50 μ g of 6-OHDA) in each lateral brain ventricle. The intracerebroventricular injections were made with a 30-gauge needle attached to a 10- μ l Hamilton syringe, at a rate of approximately 1.5 μ l/min. The injection site was 1.5 mm lateral to bregma and 3.3 mm below the dura. The syringe was left in place for 3 minutes after each injection. The pups were then warmed in a humidified box and returned to their mother two hours later. They were maintained with their mother if killed at P15, or caged in a group after weaning if killed as adults.

In situ hybridization of TH/VGLUT2 mRNA

The double *in situ* hybridization technique used for the visualization of TH and VGLUT2 mRNAs in P90 rats, normal ($n = 4$) or 6-OHDA-lesioned ($n = 4$), was the same as previously described in detail in the study of P15 rats (Dal Bo et al., 2008). The rats were anesthetized with halothane, and their brains were quickly dissected out, immersed in cold

phosphate-buffered saline (PBS; 50 mM, pH 7.4), and cut into two parts at the level of the median eminence. The rostral part containing the striatum was fixed by immersion in 4% paraformaldehyde (PFA) solution for 48 hours and processed for TH immunohistochemistry as described below. The caudal part containing the mesencephalon was immersed in frozen isopentane and stored at -80°C until processing for in situ hybridization.

$[^{35}\text{S}]\text{UTP}$ -labeled VGLUT2 probes and a nonradioactive digoxigenin (Dig)-labeled TH probe were prepared as described previously (Dal Bo et al., 2008). To generate the VGLUT2 probes, complementary RNA (cRNA) was synthesized from pCRII-Topo plasmids containing a 539-base-pair fragment of VGLUT2 cDNA (nucleotides 386–924; GenBank accession No. NM 053427). An antisense probe was produced by linearization of the plasmid using the Not I restriction enzyme and SP₆ polymerase and synthesized with the Promega riboprobe kit (Promega, Madison, WI) and $[^{35}\text{S}]\text{UTP}$ (Perkin-Elmer, Mississauga, ON, Canada). To produce the sense probe, the HindIII restriction enzyme was used to linearize the plasmid, and the probe was synthesized with T₃ polymerase. These labeled probes were purified with Mini-QuickSpin RNA columns (Roche Diagnostics, Laval, QC, Canada). The Dig-labeled TH probe was generated as previously described (Cossette et al., 2004) from a 300-base-pair PstI-EcoRI restriction fragment of rat TH cDNA (nucleotides 1279–1518; GenBank accession No. M 10244.1) contained in the pSP65 vector and linearized with HindIII. This antisense probe was synthesized with a T7 RNA polymerase. The radiolabeled VGLUT2 (2×10^6 cpm) and the Dig-labeled TH (20 ng/ml) probes were included simultaneously in the hybridization solution.

Double in situ hybridization was carried out on cryosections of the mesencephalon (12- μm -thick) fixed in 4% PFA. The TH probe was visualized with anti-Dig antibody and a Dig detection kit (Roche Diagnostic), and the VGLUT2 probe by coating autoradiography with LM-1 photographic emulsion (Amersham, ON, Canada). Slides used to compare the dual labeling between normal and 6-OHDA-lesioned rats were systematically processed together. The sections were examined under brightfield illumination with an Olympus IX-50 microscope (Carsen Group, Markham, ON, Canada) at $\times 400$ magnification. Background labeling was measured and found to be 0.37–0.53 silver grains per 500 μm^2 of section. As in previous studies (Kawano et al., 2006), TH-Dig-positive cells (DA neurons) were considered to be labeled for VGLUT2 mRNA if displaying three times the background level, i.e., at least six silver grains per cell body (Gratto and Verge, 2003). Singly and doubly labeled cells were counted in five sections per rat, between stereotaxic planes -5.28 mm and -6.24 mm from bregma (Paxinos and Watson, 2005), within the VTA and SN, pars compacta (SNc). In total, 3,894 neurons displaying TH mRNA were counted in the four normal rats: 1,727 in VTA and 2,167 in SNc; 493 were counted in the four lesioned rats: 342 in the VTA and 151 in SNc.

To verify the extent of the 6-OHDA lesion in these same rats, the rostral brain specimens containing the striatum were processed for TH immunohistochemistry. After 48 hours of fixation in PFA, 24- μm -thick transverse sections were cut with a vibratome (Leica Microsystems, Nussloch, Germany) and sequentially incubated in 5% normal goat serum solution containing 10% BSA and 0.1% Triton X-100 for 1 hour, in mouse

monoclonal TH antibody (clone TH-2; Sigma) diluted 1:1,000 in PBS overnight and in biotinylated anti-mouse antibodies (Jackson ImmunoResearch, West Grove, PA) diluted 1:1,000, followed by 1:1,000 streptavidin-HRP (Jackson ImmunoResearch). The peroxidase reaction was revealed with 0.05% 3,3'-diaminobenzidine tetrahydrochloride (DAB; Sigma) and hydrogen peroxide (0.01%) in Tris-HCl buffer (50 mM, pH 7.4).

TH and VGLUT2 immunocytochemistry

Rats were deeply anesthetized with sodium pentobarbital (80 mg/kg, i.p.) and fixed by intracardiac perfusion of a solution of 3% acrolein (50 ml for P15 rats; 250 ml for P90 rats) in 0.1 M phosphate buffer (PB, pH 7.4), followed by 4% PFA in the same buffer (150 ml for P15 rats; 300 ml for P90 rats). The brain was removed, postfixed by immersion in the PFA solution at 4°C (2 hours for P15 rats; 1 hour for P90 rats), and washed in phosphate-buffered saline (PBS: 0.9% NaCl in 50 mM PB, pH 7.4). Fifty-micrometer-thick transverse sections at the level of SN and nAcb were then cut in PBS with a vibratome (VT100S; Leica), immersed in 0.1% sodium borohydride (Sigma) in PBS for 30 minutes at room temperature, and washed in this buffer before further processing.

Antibodies characterization. Mouse anti-TH (clone TH-2; No. T1299; Sigma) and/or rabbit anti-VGLUT2 (No. 135 403; Synaptic Systems, Goettingen, Germany) antibodies were used. As described by Sigma, this particular monoclonal anti-TH antibody is derived from a hybridoma produced by the fusion of mouse myeloma cells and splenocytes from a mouse immunized against whole-rat TH protein (Haycock, 1993). It recognizes an epitope (~ 60 kDa, amino acids 9–16) present in the N-terminal region of both rodent and human TH and has previously been used in combined immunocytochemical and in situ hybridization experiments to detect VGLUT2 mRNA in mesencephalic DA neurons (Kawano et al., 2006). In the present study, the immunostaining specificity of this antibody toward DA neurons was evidenced not only by the topographic distribution of immunoreactive cell bodies and axon terminals in the different rat brain regions examined (see Hökfelt et al., 1984), but also by their near-total disappearance from the SN and NStr after neonatal 6-OHDA lesion.

As described by Synaptic Systems, the polyclonal anti-VGLUT2 antibody was raised in rabbit against a Strep-Tag fusion protein from the C-terminal domain of the predicted sequence of rat vesicular glutamate transporter 2 (amino acids 510–582; Takamori et al., 2001). The immunocytochemical specificity of this particular antibody has been demonstrated by Western blot analysis of homogenized rat brains and/or crude synaptic vesicle fractions from rat brain, in which a single broad band slightly above 60 kDa was found, and by preadsorption experiments with the GST fusion protein used as immunogen, in which the immunostaining of rat brain sections was completely eliminated (see references in Persson et al., 2006; see also Takamori et al., 2001; Zhou et al., 2007).

TH immunolabeling for light microscopy. To ensure a successful visualization of mesencephalic DA neurons in these rats and to verify the extent of their lesioning and of the DA neoinnervation in SN after neonatal 6-OHDA, tissue to be processed for electron microscopy after dual TH and VGLUT2 labeling was first examined by light microscopy after immunolabeling for only TH. At room temperature, sections were preincubated for 1 hour in a blocking solution containing 5% normal goat serum, 0.3% Triton X-100, and 0.5% gelatin in

TABLE 1. Primary Antibodies

| Antigen | Immunogen | Information | Dilution used |
|-----------------------------------|---|--|------------------------|
| Tyrosine hydroxylase | Clone TH-2, aa 9-16 from N-terminal of rat | Sigma (St. Louis, MO), mouse monoclonal, No. 1299 | LM 1:1,000 EM 1:500 |
| Vesicular glutamate transporter 2 | Fusion protein, aa 510-582 from C-terminal of rat | Synaptic Systems (Göttingen), rabbit polyclonal, No. 135 403 | EM 1:500 |

PBS and incubated overnight in a 1:1,000 dilution of TH antibodies and then for 2 hours in a 1:1,000 dilution of biotinylated goat anti-mouse (for TH) IgGs (Jackson ImmunoResearch) in blocking solution. After rinses in PBS (3 × 10 minutes), they were incubated for 1 hour in a 1:1,000 dilution of horseradish peroxidase (HRP)-conjugated streptavidin (Jackson ImmunoResearch), washed in PBS, and incubated for 2–5 minutes in TBS containing 3,3'-diaminobenzidine tetrahydrochloride (0.05% DAB) and hydrogen peroxide (0.02%). The reaction was stopped by several washes in TBS followed by PB, and the sections were mounted on microscope slides, dehydrated in ethanol, cleared in toluene, and coverslipped with DPX. They were examined and photographed with a Leitz Diaplan optical microscope coupled to a Spot RT color digital camera with Spot v4.0.5 for Windows (Diagnostic Instruments, Sterling Heights, MI). These images were adjusted for brightness, contrast, and sharpness in Adobe Photoshop.

Double TH/VGLUT2 immunolabeling for electron microscopy. Sections were preincubated as described above, except for omission of Triton X 100 in the blocking solution, and then incubated for 48 hours, at room temperature, in a 1:500 dilution of both primary TH and VGLUT2 antibodies (Table 1). After rinses in PBS, they were then placed overnight, at room temperature, in a 1:50 dilution of goat anti-rabbit IgGs conjugated to 1-nm colloidal gold particles (AuroProbe One; Amersham, Oakville, Ontario, Canada) and treated with an IntenSE kit (Amersham) for 15 minutes to increase the size of immunogold particles. The immunogold-labeled sections were then processed for TH with the immunoperoxidase technique as described above.

Immunocytochemical controls included double immunocytochemical processing, but without either one or both primary antibodies. Only the expected single labeling was then observed after omitting one of the primary antibody, with no labeling whatsoever in the absence of both of them.

Further processing for electron microscopy was as previously described in detail by Riad et al. (2000). In brief, sections were osmicated, dehydrated, and flat embedded in Durcupan resin (Sigma) between a glass slide and a plastic coverslip (Rinzl; Thomas Scientific, Swedesboro, NJ). After 48 hours of polymerization at 60°C, the coverslips were removed, and specimens from the regions of interest (nAcb, NStr, and SN), were excised from the slides and glued at the tip of resin blocks. Ultrathin sections were then cut with an ultramicrotome (Reichert Ultracut S; Leica Canada, Montreal, Québec, Canada), collected on bare square-meshed copper grids, stained with lead citrate, and examined with an electron microscope (Philips CM100; Philips Electronics, St.-Laurent, QC, Canada).

Quantitative analysis of electron microscopic data.

Three brain regions were examined in P15 (n = 14) and P90 rats (n = 16) subjected or not to the neonatal 6-OHDA lesion at P4: the core of nAcb, at transverse levels corresponding to A 10.8–11.28 mm in the stereotaxic atlas of Paxinos and Watson (2005), a central portion of the dorsal striatum at this same transverse level, and a small piece of mesencephalic tissue located at mid-distance between the midline and the lateral border of the ventral tegmentum, in a location corresponding to the remnants of SN, pars compacta and reticulata, at transverse levels corresponding to A 2.9–3.8 mm (Paxinos and Watson, 2005). Doubly immunolabeled material from the nAcb was examined in seven normal and seven 6-OHDA-lesioned rats, aged 15 days (body weight 15–20 g), and in eight normal and eight 6-OHDA-lesioned rats, aged 90 days (300–400 g). In each of these rats, at least 50 electron micrographs were obtained from a narrow area of thin section less than 10 μm away from the tissue–resin border, at working magnifications ranging from ×3,000 to ×15,000. The film negatives were scanned (Epson Perfection 3200), converted into positive pictures, and adjusted for brightness and contrast in Adobe Photoshop before printing.

Most immunolabeled profiles could then be positively identified as axon varicosities, i.e., axon dilations (>0.25 μm in transverse diameter) containing aggregated small vesicles, often one or more mitochondria, and displaying or not a synaptic membrane specialization (junctional complex). The immunoperoxidase labeling was in the form of a more or less dense, fine precipitate, often outlining the small vesicles or mitochondria and the plasma membrane of varicosities. Only axon varicosity profiles decorated with three or more silver-intensified gold particles were considered as immunogold labeled. Smaller immunolabeled profiles were assumed to represent intervaricose segments of unmyelinated axons.

Thirty micrographs per rat, printed at a uniform magnification of ×30,000, were selected on the basis of optimal ultrastructural preservation. In this 50,000-μm² area of thin section in each rat, singly or dually immunolabeled profiles of axon varicosities were counted and categorized as immunopositive for only TH, only VGLUT2, or both TH and VGLUT2 (TH/

Figure 1.

Low-magnification and higher magnification pictures from TH-immunostained sections taken at the same transverse level across the ventral mesencephalon, in P15 (A,A',B,B') and P90 (C,C',D,D') rats, normal (A,A',C,C') or neonatally lesioned with 6-OHDA (B,B',D,D'). These micrographs and those in Figure 2 illustrate the various conditions in which the mesencephalic TH neurons of adult rat (P90) were examined by comparison with immature rat (P15) for coexpression of VGLUT2 mRNA (Fig. 3) or colocalization of VGLUT2 protein in some of their axon terminals (varicosities; Figs. 4–8). Note that, at both ages, TH-immunostained cell bodies and dendrites were almost totally absent from the SN of 6-OHDA-lesioned rats, but were still present in appreciable numbers in the VTA. Note how the pattern of TH immunostaining in the zona reticulata of SN (framed area) differs according to age and to normal or post lesion state. In normal rats at both ages, only dendrites (and, at P15, a few cell bodies still migrating toward their final destination) are seen in this part of SN. In the 6-OHDA-lesioned rats, TH-immunostained dendrites are no longer visible in the zona reticulata, but fine, varicose TH immunostained fibers may be observed to have pervaded this region at P15 and to have developed into a relatively dense axonal reinnervation at P90 (for further description and illustration see Fernandes Xavier et al., 1994). Scale bars = 1 mm in D (applies to A–D); 200 μm in D' (applies to A'–D').

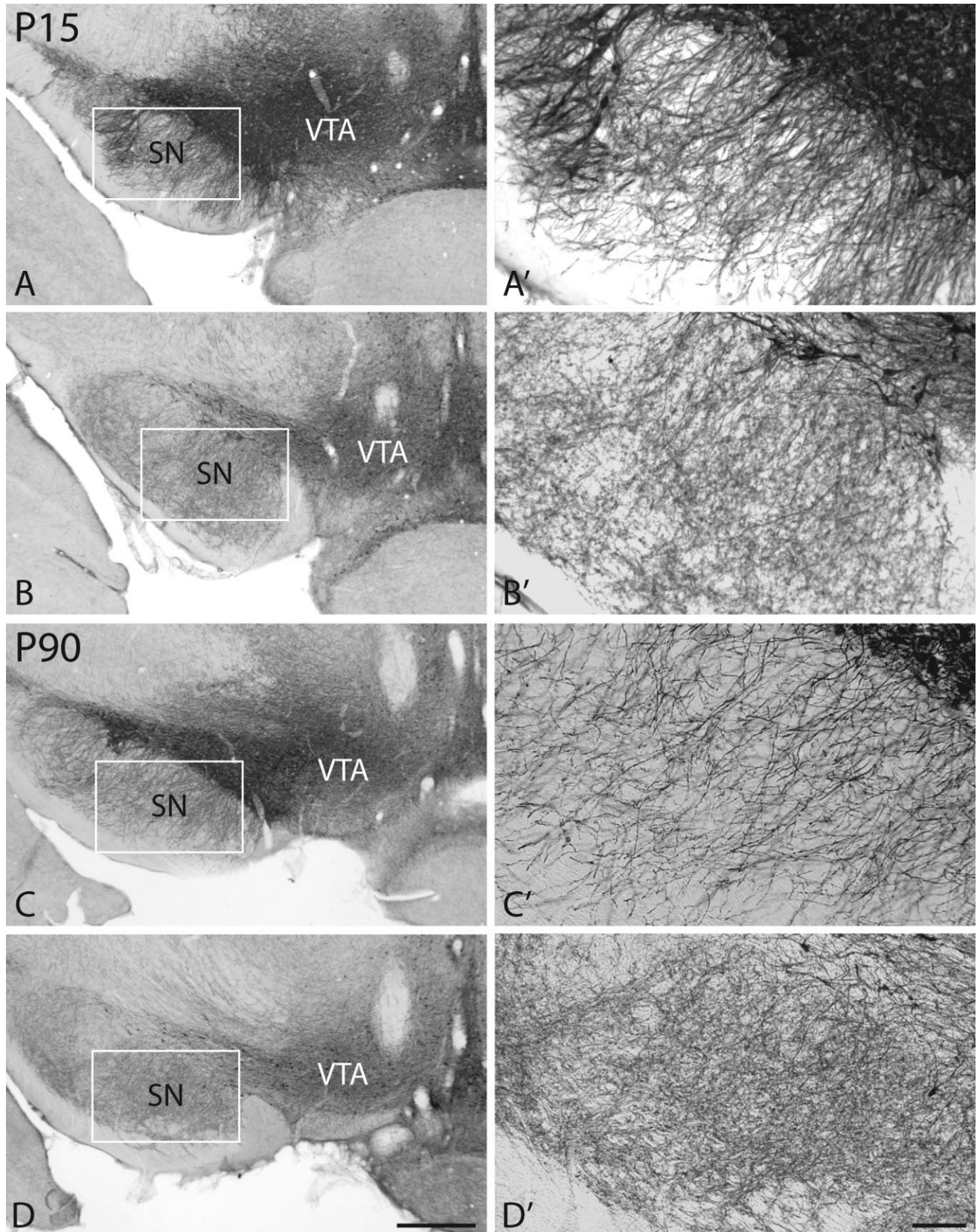
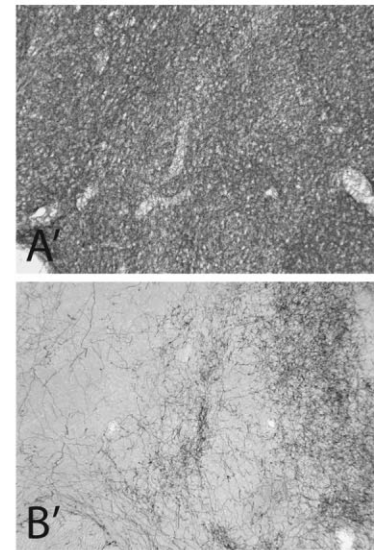
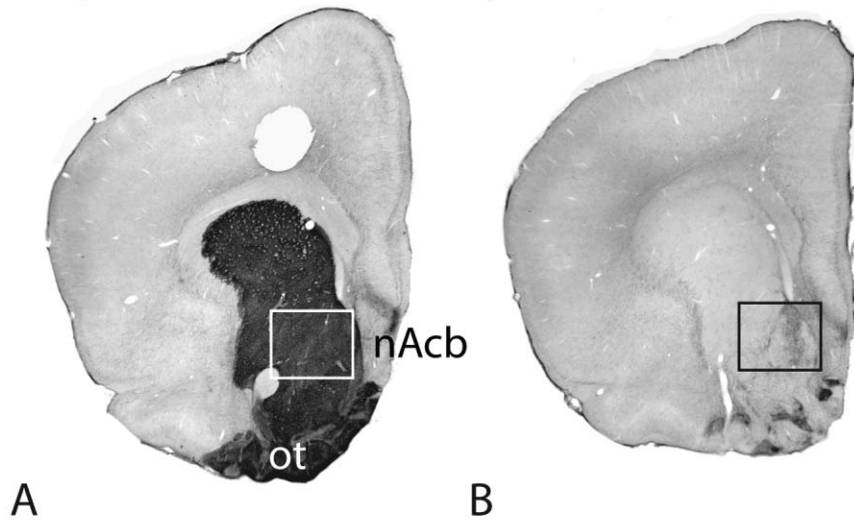


Figure 1

P15



P90

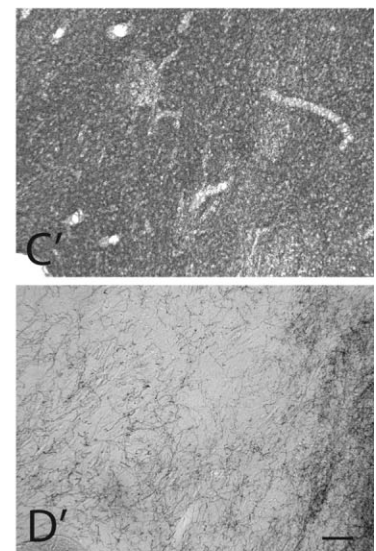
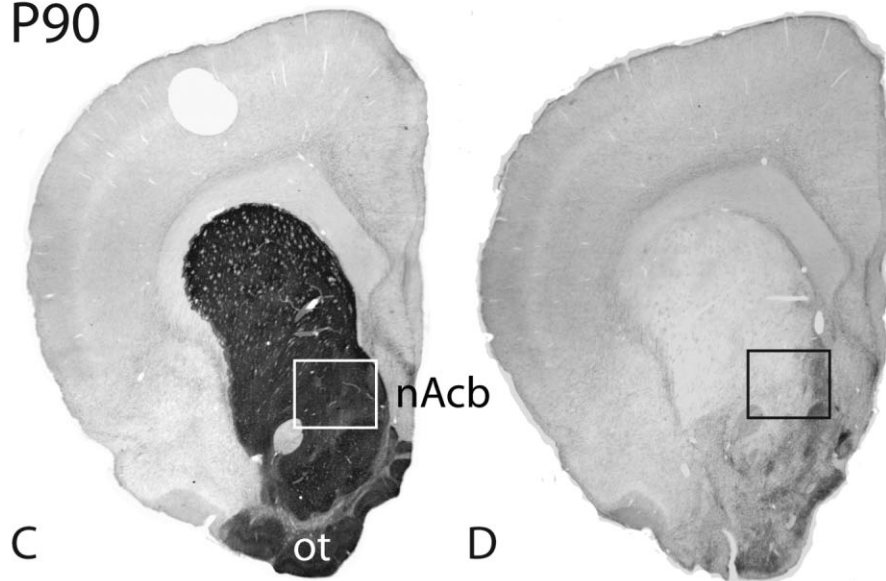


Figure 2. Micrographs from TH-immunostained sections at a more rostral transverse level than in Figure 1, illustrating the nAcb and NStr in P15 (A,A',B,B') and P90 (C,C',D,D') rats, normal (A,A',C,C') or neonatally lesioned with 6-OHDA (B,B',D,D'). The low-magnification pictures illustrate the almost total disappearance of DA (TH-immunostained) innervation in the NStr, but the persistence of a significant number of TH-immunostained terminals in the nAcb (as well as in the olfactory tubercle; ot) of 6-OHDA-lesioned rats (B,D). This is also apparent in the higher magnification views of the nAcb (A'–D'). Scale bar = 200 μ m.

VGLUT2). In normal rats, 1,699 axon terminals in total were thus examined at P15, and 1,290 at P90. In rats neonatally lesioned with 6-OHDA, 1,021 axon terminals were examined at P15 and 986 at P90. Because the same thin section surface was being examined in each rat, these counts could be expressed as means \pm SEM per rat, for statistical comparison of the various types of labeling between normal and lesioned rats of the same age.

The varicosity profiles were then measured for long (L) and short (s) axes and mean diameter $(L + s/2)$, in the public-domain Image J processing software from NIH, and classified as showing or not a synaptic junction, i.e., a localized straightening and thickening of apposed plasma membranes on either side of a slightly widened extracellular space. The length of junctional complexes was measured, and the synaptic frequency observed in single sections was extrapolated to the

TABLE 2. Number and Proportion of Neurons Coexpressing TH and VGLUT2 mRNA in the Ventral Tegmental Area and Substantia Nigra of Normal and 6-OHDA-Lesioned Immature (P15) and Mature (P90) Rats¹

| | TH total | | TH/VGLUT2 | | TH/VGLUT2 (%) | |
|--------------|------------------------|---------------------|-----------------------|-----------|-------------------------|--------------------------|
| | P15 | P90 | P15 | P90 | P15 | P90 |
| Normal | | | | | | |
| Total number | 2,775 | 3,894 | 25 | 46 | | |
| VTA | 102 ± 7 | 86 ± 9 | 1.8 ± 0.3 | 2 ± 0.3 | 1.8 ± 0.3 | 2.4 ± 0.5 |
| SN | 152 ± 12 | 109 ± 4 | 0.7 ± 0.4 | 0.3 ± 0.1 | 0.4 ± 0.2 | 0.3 ± 0.1 |
| 6-OHDA | | | | | | |
| Total number | 152 | 493 | 36 | 26 | | |
| VTA | 39 ± 5 ⁴ | 17 ± 2 ³ | 10.3 ± 1 ⁴ | 1.3 ± 0.4 | 26.3 ± 2.5 ⁴ | 7.2 ± 1.5 ^{2,5} |
| SN | 4.6 ± 2.6 ⁴ | 8 ± 2 ⁴ | 0 | 0 | 0 | 0 |

¹Total number counted and mean ± SEM for the number of neurons per section (three or four sections per rat at P15 and 5 sections per rat at P90) in four rats at each age. At right, the number of dually labeled neurons (TH/VGLUT2) is expressed as a percentage of all neurons containing TH mRNA (TH total). The data at P15 are from Dal Bo et al. (2008).

² $P < 0.05$ for 6-OHDA-lesioned vs. normal rats of the same age.

³ $P < 0.01$ for 6-OHDA-lesioned vs. normal rats of the same age.

⁴ $P < 0.001$ for 6-OHDA-lesioned vs. normal rats of the same age.

⁵ $P < 0.001$ for P90 vs. P15 rats.

whole volume of varicosities by means of the stereological formula of Beaudet and Sotelo (1981; see also Umbriaco et al., 1994).

A similar analysis was carried out on doubly labeled material from the NStr of three of the 15-day-old and three of the 90-day-old normal rats, and from the SN of three of the 15-day-old and three of the 90-day-old 6-OHDA-lesioned rats; 50,000 μm^2 of thin section was again examined in each rat, for a total of 468 immunolabeled terminals at P15 and 550 at P90 in the NStr of normal rats, and of 286 axon immunolabeled terminals at P15 and 201 at P90 in the SN of 6-OHDA-lesioned rats. In the SN, care was taken to restrict the analysis to axon terminals, excluding rare cell bodies or occasional TH-, VGLUT2-, or TH/VGLUT2-labeled dendrites, which were generally much larger, contained the typical array of microtubules, and were often contacted by synaptic terminals.

Statistical analysis

All data were expressed as group mean ± SEM. Statistical analyses were performed in GraphPad Prism 4. One-way ANOVA and unpaired Student's *t*-tests were used to determine statistical significance. *P* values below 0.05 were considered statistically significant. Because in situ hybridization was performed on frozen tissue sections, it was deemed meaningful to compare the number of cells singly or dually labeled for TH and VGLUT2 mRNA, not only between normal and lesioned rats at each age, but also between P15 and P90 rats. However, fixed immature and mature rat brain tissue may not be equally permeable to immunoreagents. Therefore, the numbers of axon terminals in each category of immunolabeling were not compared between P15 and P90 rats.

RESULTS

Distribution of TH immunoreactivity in P15 and P90 rats, normal or subjected to neonatal 6-OHDA lesion

As visualized by light microscopy, the pattern of TH immunostaining in normal rats was entirely consistent with earlier TH or DA immunocytochemical descriptions of the distribution of mesencephalic DA neuron soma-dendrites and axon terminals at both ages examined (Antonopoulos et al., 2002; Hökfelt et al., 1984; Voorn et al., 1988). As previously reported (Hanaway et al., 1971; Voorn et al., 1988), at P15, all DA cell

bodies were not yet tightly grouped in the pars compacta of SN, and many were still present in the pars reticulata (Fig. 1). However, in both NStr and nAcb, the DA innervation appeared to be already as dense at P15 as at P90 (compare Fig. 2A and C).

Also in keeping with earlier observations, after neonatal 6-OHDA lesion, there was an almost total disappearance of TH-positive soma-dendrites in the pars compacta and reticulata of SN and of TH axon terminals in the NStr, which appeared to be complete at P15. In contrast, even if some cell loss was also apparent in VTA, TH cell bodies were still visible in this region, as well as some TH axon terminals in both the core and the shell of nAcb (Fig. 2B,D). There were no indications of DA terminal sprouting in either NStr or nAcb at P90. However, as first reported by Fernandes Xavier et al. (1994), in the lesioned rats, there was a striking DA neoinnervation of the remnants of SN, pars compacta and reticulata, by fine, varicose, axon-like, TH-immunoreactive processes, which were already numerous at P15, and even more abundant at P90 (Fig. 1B'-D').

Coexpression of TH and VGLUT2 mRNA in mesencephalic neurons of P15 and P90 rats, normal or subjected to neonatal 6-OHDA lesion

As previously observed in normal P15 rats, there were only few neurons expressing both TH and VGLUT2 mRNA in the VTA and SNc of normal P90 rats (Table 2), and these neurons were only weakly labeled for VGLUT2 mRNA compared with presumptive glutamatergic neurons in neighboring anatomical regions such as the red nucleus (Supp. Info. Fig. 1). As also illustrated in Supporting Information Figure 1, there was no cell labeling whatsoever in material processed with sense probes.

As had been seen at P15, the total number of neurons displaying only TH mRNA was markedly reduced in the VTA of adult (P90) 6-OHDA-lesioned rats ($P < 0.01$), and such neurons had almost totally disappeared from the SNc (Table 2, Fig. 3). At P15, the proportion of VTA neurons coexpressing TH and VGLUT2 mRNA had been found to be significantly higher in 6-OHDA-lesioned compared with control rats, amounting to 26.3% compared with 1.8% of all TH mRNA-positive neurons ($P < 0.001$). At P90, the proportion of dually labeled VTA neurons was also higher after the neonatal lesion than in controls ($P < 0.05$), but considerably lower than at P15

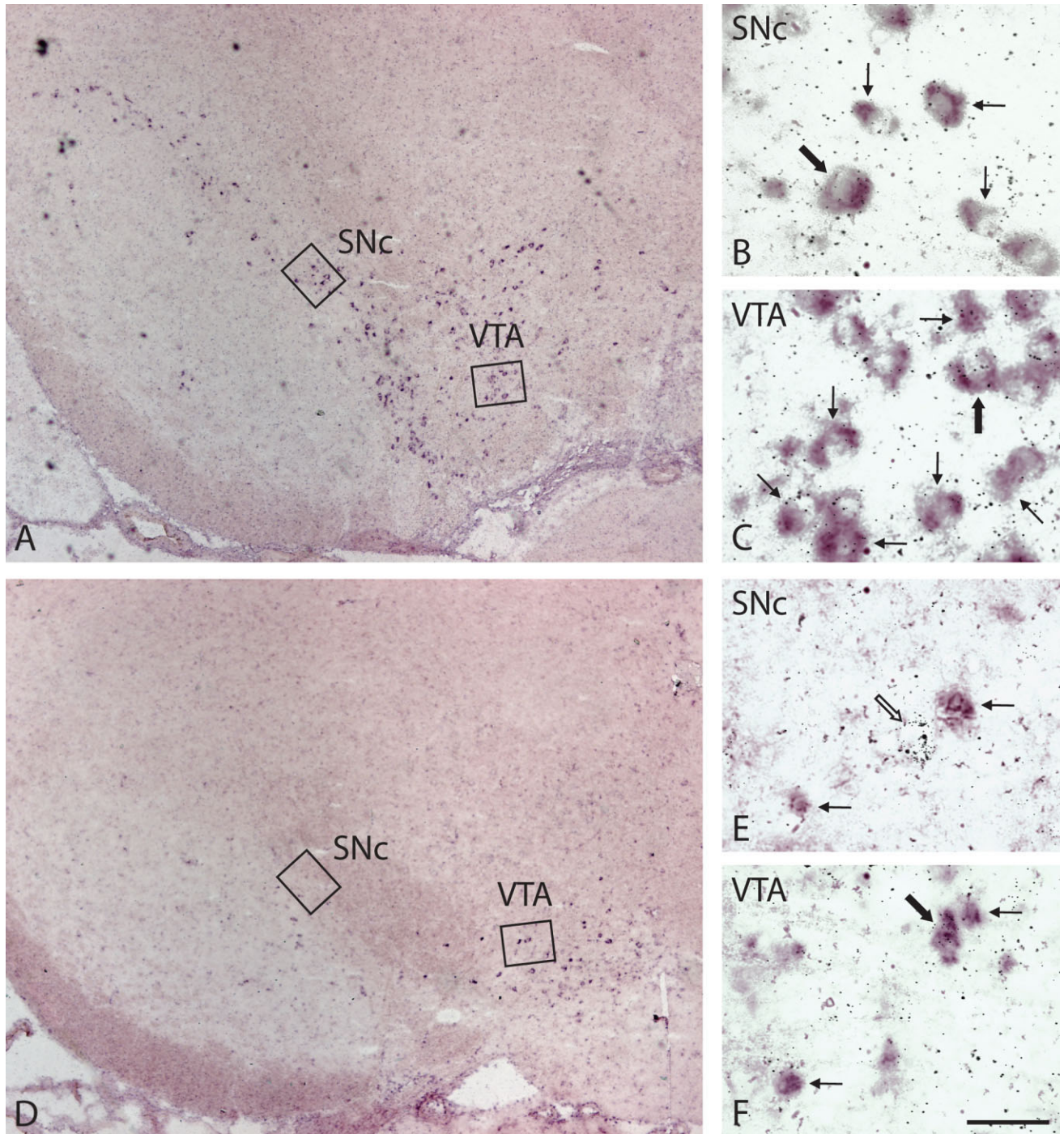


Figure 3. Expression of TH and VGLUT2 mRNAs in SNc and VTA neurons of 90-day-old normal (A–C) or neonatally 6-OHDA-lesioned (D–F) rats. Double in situ hybridization with DIG label and radiolabel to detect TH mRNA (purple) and VGLUT2 mRNA (silver grains), respectively. A,D: Low-power micrographs from normal (A) and 6-OHDA-lesioned rat (D) illustrating the effects of the 6-OHDA lesion. At this low magnification, the silver grain labeling of VGLUT2 mRNA is barely visible, but there is an almost total disappearance of the TH mRNA labeling in the SNc and a considerable reduction of this labeling in the VTA, as a result of the 6-OHDA lesion. In B,C, coexpression of TH and VGLUT2 mRNA is observed in a few neurons of the SNc and VTA of normal rats (thick arrows). In 6-OHDA-lesioned rats, there are no neurons expressing both TH and VGLUT2 mRNA in the remnants of the SNc (E), but some surviving DA neurons coexpress VGLUT2 mRNA in the VTA (thick arrow in F). Some neurons expressing only VGLUT2 are present in the SNc and VTA of both normal and 6-OHDA-lesioned rats, as exemplified in E (open arrow). Scale bar = 25 μ m.

($P < 0.001$), with only 7.2% of all TH mRNA-positive neurons also labeled for VGLUT2 mRNA.

TH-, VGLUT2-, and TH/VGLUT2-immunoreactive axon terminals in the nAcb of P15 and P90 rats, normal or subjected to neonatal 6-OHDA lesion

As also reported previously in P15 rats, and illustrated here in Figure 4A,B, axon terminals labeled for TH or VGLUT2 were readily identified in the nAcb of both normal and 6-OHDA-lesioned rats at P90 (Fig. 4C,D). Whereas a significant number of TH/VGLUT2-labeled terminals had been previously found in both normal and 6-OHDA-lesioned rats at P15 (e.g., Figs. 5A,B, 6A–D), none was seen in the eight normal P90 rats and only 6 in the eight neonatally lesioned P90 rats (Figs. 5C–E, 6E–H).

As shown in Table 3, VGLUT2 was colocalized with TH in 28% of all TH-labeled axon terminals in the nAcb of normal P15 rats. After the neonatal 6-OHDA lesion, the average number of all TH-labeled terminals was markedly decreased ($P < 0.001$), but the proportion that was also labeled for VGLUT2 slightly but significantly increased (37%; $P < 0.05$). The apparent decrease in the mean number of terminals labeled for VGLUT2 only was not statistically significant ($P = 0.15$). In P90 rats, the number of axon terminals labeled for TH only was also decreased after the neonatal 6-OHDA lesion ($P < 0.001$), without a significant change in the number of terminals labeled for only VGLUT2. Only six TH/VGLUT2-labeled terminals were seen in the eight rats neonatally lesioned with 6-OHDA.

Ultrastructural features of TH-, VGLUT2-, and TH/VGLUT2-immunoreactive axon terminals in the nAcb of P15 and P90 rats, normal or subjected to neonatal 6-OHDA lesion

The intrinsic and relational features of the singly or dually labeled terminals in the nAcb of normal and 6-OHDA-lesioned rats at P15 and P90 are summarized in Table 4 and illustrated in Figures 4–6. There were no significant differences in size between axon terminals labeled for only TH in normal and 6-OHDA-lesioned rats at either age. In contrast, in both normal and 6-OHDA-lesioned rats, the size of terminals labeled for VGLUT2 only showed a significant and comparable increase between P15 and P90. In both normal and 6-OHDA-lesioned P15 rats, the terminals dually labeled for TH/VGLUT2 were comparable in size to those labeled for VGLUT2 only and were significantly larger than those labeled for TH only ($P < 0.05$). At P90, and in both normal and 6-OHDA-lesioned rats, the terminals labeled for VGLUT2 only were also significantly larger than those labeled for TH only. The length of synaptic junctions formed by terminals labeled for VGLUT2 only also showed a significant increase between P15 and P90 in both normal and 6-OHDA-lesioned rats.

As extrapolated stereologically from the observations in single thin sections, the synaptic incidence of nAcb axon terminals labeled for TH only was relatively low, but was greater at P15 than P90, whether in normal (37% vs. 7%) or in 6-OHDA-lesioned (70% vs. 22%; Table 4) rats. The synaptic incidence of terminals labeled for VGLUT2 only was also relatively low in both normal (58%) and 6-OHDA-lesioned rats (71%) at P15, whereas, at P90, most if not all such varicosities appeared to be synaptic (96% and 106% in normal and 6-OHDA-lesioned rats, respectively).

The synaptic incidence extrapolated for TH/VGLUT2-immunoreactive varicosities in normal and 6-OHDA-lesioned P15 rats was also greater than 100% (110% and 130%), suggesting that all these dually labeled terminals were synaptic, with a significant number making more than a single synaptic contact (e.g., Figs. 5C, 6E). When the terminals labeled for only TH were pooled with those dually labeled for TH/VGLUT2, the synaptic incidence for all TH-positive terminals at P15 was 57% in normal rats and 92% after the neonatal 6-OHDA lesion ($P > 0.001$).

TH-, VGLUT2-, and TH/VGLUT2-immunoreactive axon terminals in the NStr of normal P15 and P90 rats

In view of the near-absence of DA terminals in the NStr after neonatal 6-OHDA lesion, the ultrastructural features of axon terminals labeled for TH, VGLUT2, or TH/VGLUT2 in this region were examined only in normal P15 and P90 rats (Table 4, Fig. 7). In the P15 rats, an average of 80 ± 12 terminals per rat were labeled for TH only, 58 ± 19 for VGLUT2 only, and 17 ± 6 for TH/VGLUT2 (17% of all TH terminals), whereas, in P90 rats, 115 ± 5 terminals per rat were labeled for TH only and 68 ± 8 for VGLUT2 only. Not a single dually labeled terminal was found in the NStr of P90 rats.

As in nAcb, the neostriatal axon terminals labeled for TH only were of the same size at P15 and P90 and significantly smaller than those labeled for TH/VGLUT2 at P15 ($P < 0.05$) or for VGLUT2 only at P90 ($P < 0.01$). In NStr, however, there was no apparent increase in size of the VGLUT2 terminals between P15 and P90, nor was the average length of junctions made by these terminals significantly different at the two ages.

The synaptic incidence of NStr terminals in the various categories of labeling is shown in Table 5. Again, terminals labeled for TH only were not often synaptic but were more frequently so at P15 (18%) than at P90 (6%; $P < 0.01$). Terminals labeled for VGLUT2 only were much more frequently synaptic than the terminals labeled for TH only ($P < 0.001$ at P15 and $P < 0.01$ at P90), but not all synaptic at P15 (70%) as opposed to P90 (99%). TH/VGLUT2 terminals at P15 also appeared to be mostly if not all synaptic (93%; $P < 0.01$ vs. TH only), raising the synaptic incidence for all TH-positive terminals (TH + TH/VGLUT2) to 31% at this age compared with the 6% value at P90 ($P < 0.001$).

DA neoinnervation in SN of P15 and P90 rats subjected to neonatal 6-OHDA lesion

As illustrated in Figure 8, in both P15 and P90 rats, many of the TH- as well as VGLUT2-immunoreactive profiles in the SN remnants after neonatal 6-OHDA lesion could be positively identified as axon varicosities (terminals), according to conventional morphological criteria (Peters and Palay, 1996; see also Materials and Methods). In the three rats examined at each age, TH/VGLUT2-labeled varicosities were also found at P15 but not at P90. The average number of immunoreactive terminals per rat was 29 ± 12 for TH only, 44 ± 17 for VGLUT2 only, and 22 ± 6 for TH/VGLUT2 (46% of all TH terminals) at P15, whereas, at P90, the corresponding numbers were 20 ± 3 for TH only and 47 ± 3 for VGLUT2 only.

Here, again, terminals labeled for TH only or for VGLUT2 only did not differ in size between P15 and P90, but, at P90,

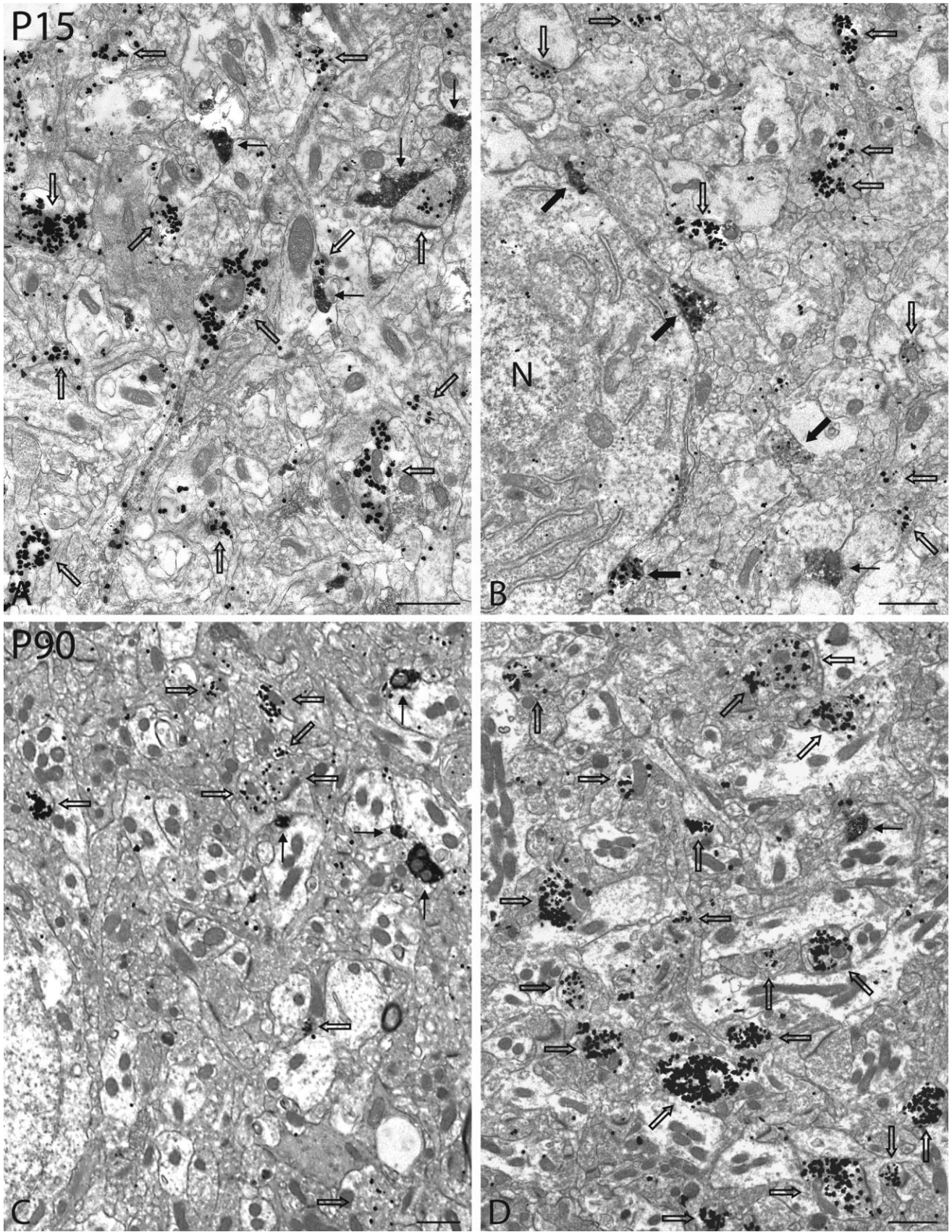


Figure 4. Low-magnification electron micrographs illustrating immunoreactive axon terminals (varicosities) in the nAcb of P15 (A,B) and P90 (C,D) rats, normal (A,C) or neonatally lesioned with 6-OHDA (B,D), after dual immunolabeling for TH and VGLUT2. In this and the following figures, TH and VGLUT2 were labeled with the immunoperoxidase technique (fine DAB precipitate) and the immunogold technique (silver intensified, immunogold particles), respectively, and varicosities were labeled for only TH, only VGLUT2, and both TH/VGLUT2, designated by thin arrows, open arrows, and thick arrows, respectively. In the small area illustrated in A (P15, normal rat), only varicosities singly labeled for TH or VGLUT2 are visible, whereas, in B (P15, 6-OHDA-lesioned rat), several dually TH/VGLUT2-labeled varicosities (thick arrows), in addition to singly labeled ones, may be observed. Three of these four doubly labeled terminals are closely apposed to a neuronal cell body (N in nucleus). In adult rats (C,D), singly labeled TH and VGLUT2 varicosities are seen in both the normal and the 6-OHDA-lesioned rat, but no dually labeled ones. Also note the reduced number of only TH varicosities in B and D (6-OHDA-lesioned rat) compared with A and C (normal rat). Scale bars = 1 μ m.

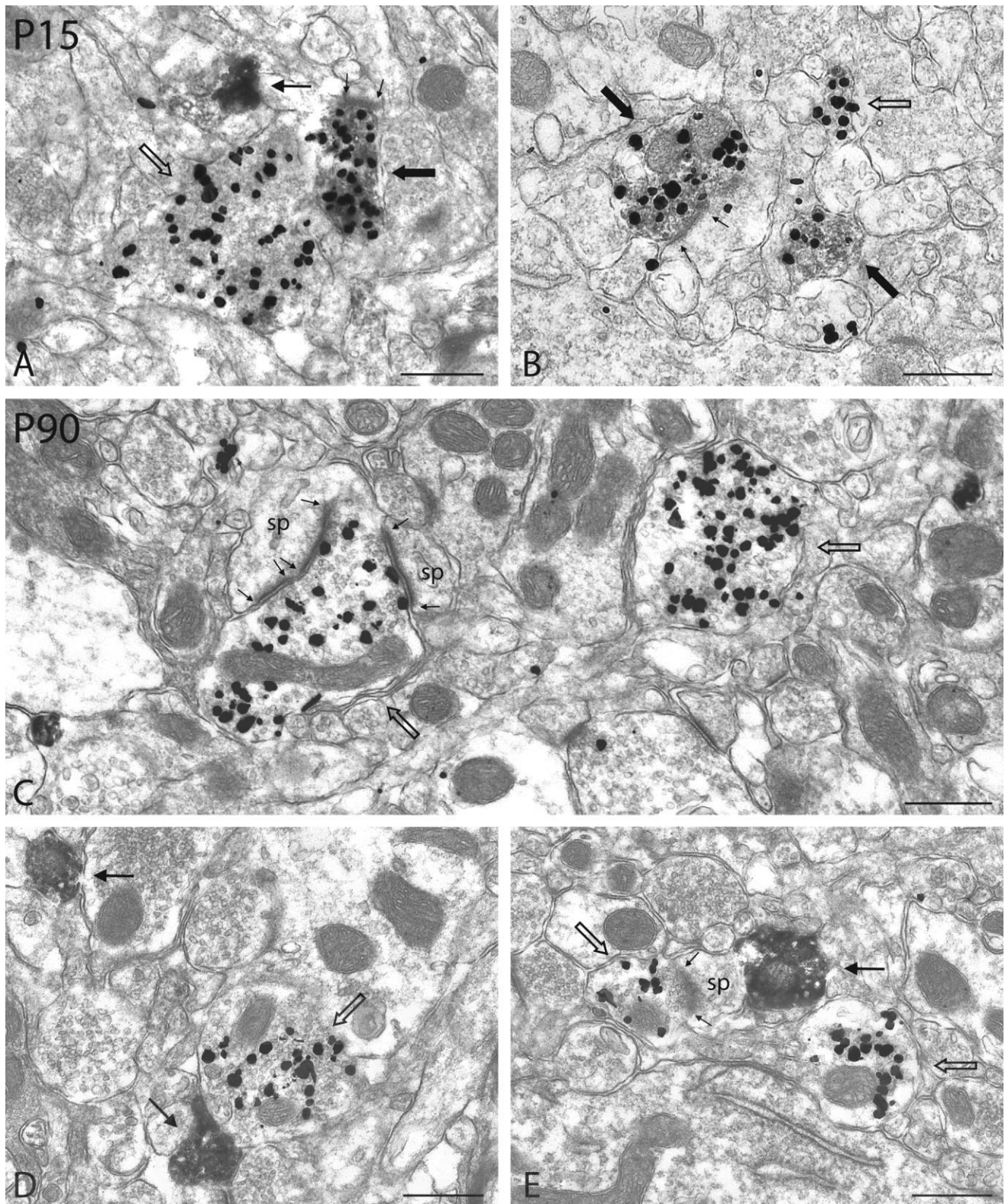


Figure 5.

Higher magnification views of immunoreactive axon terminals in the nAcb of P15 and P90 normal rats, after dual immunolabeling for TH (immunoperoxidase-DAB) and VGLUT2 (immunogold). At P15 (A,B), but not P90 (C–E), dually immunolabeled terminals (thick arrows) are seen in addition to terminals singly labeled for TH (thin arrows) or VGLUT2 (open arrows). In A, a synaptic junction (between small arrows) is formed by the dually labeled terminal, which is also the case for the larger of the two dually labeled terminals in B. In C, note the two large asymmetrical synaptic contacts (between small arrows) onto dendritic spines (sp) formed by one of two nearby VGLUT2 terminals. The larger one of these contacts appears to be annular (see also Fig. 6E). In D, a VGLUT2 varicosity is directly apposed to one of two TH terminals. In E, the left-sided VGLUT2 varicosity appears to make synapse (between small arrows) onto the dendritic profile to which the TH terminal is directly apposed. Also note the generally larger size of VGLUT2- compared with TH-labeled terminals. Scale bars = 0.5 μm .

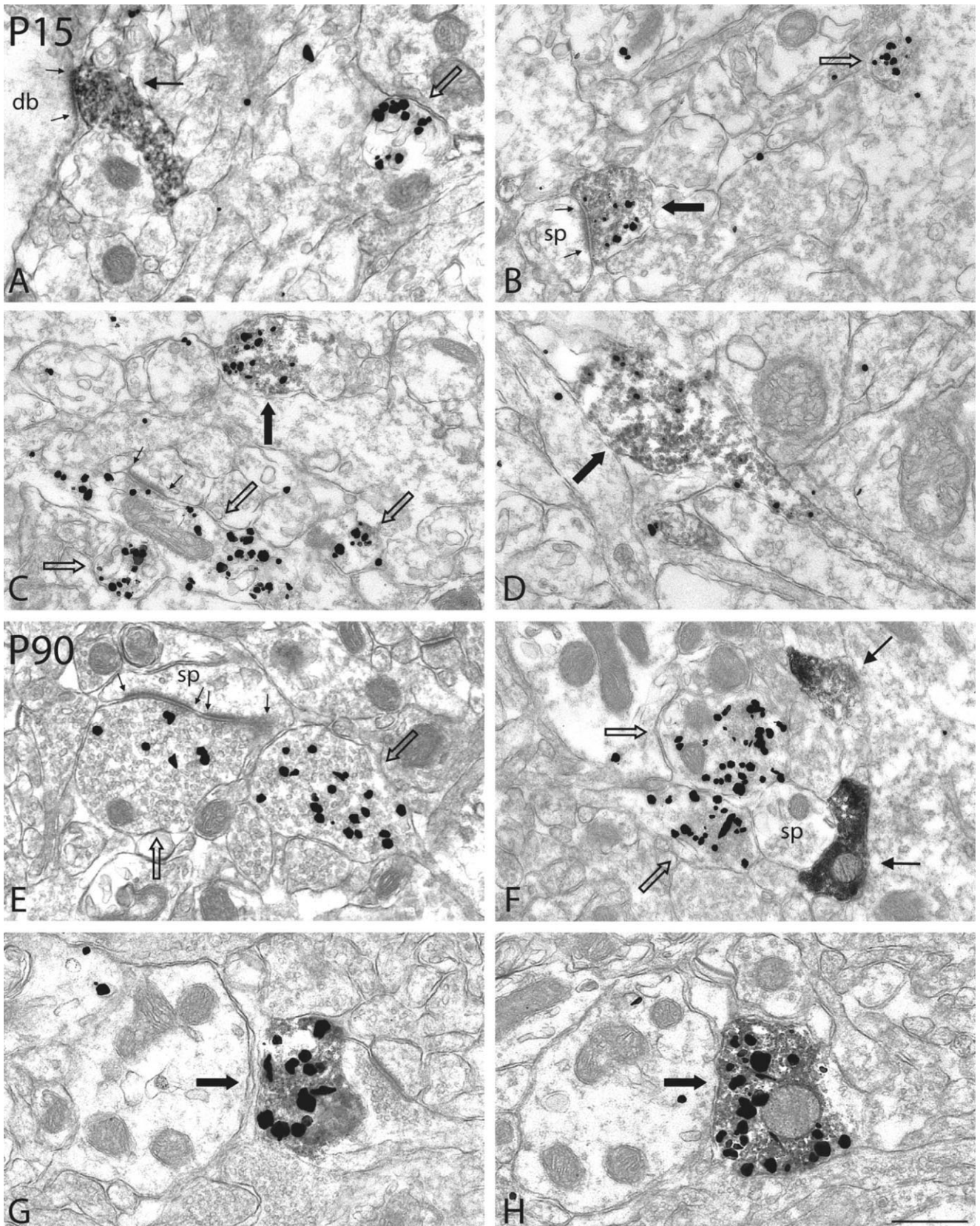


Figure 6.

Axon terminals from the nAcb of P15 (A–D) and P90 (E–H) rats neonatally lesioned with 6-OHDA, after dual immunolabeling for TH (immunoperoxidase-DAB) and VGLUT2 (immunogold). Dually immunolabeled terminals (thick arrows) were numerous at P15, in addition to terminals singly labeled for TH (thin arrows) or for VGLUT2 (open arrows). In A,B, two of these terminals are seen in synaptic junction (between small arrows) with dendritic profiles (branch, db, in A; spine, sp, in B). In C,D, the dually labeled varicosities presumably make synapse in another plane of section. The three adjacent VGLUT2 varicosities in C are directly apposed to one another, and the elongated one displays an asymmetrical synaptic junction (between small arrows). In D, the dually labeled varicosity may be observed to emerge from its thin, unmyelinated parent axon. In E,F, note the larger size of VGLUT2 compared with TH varicosities (in F) as already observed at P15. The larger of the two VGLUT2 varicosities in E forms a wide annular, asymmetrical synaptic specialization (between small arrows) on a dendritic spine (sp), as was seen in Figure 5C. In F, the two VGLUT2 varicosities are directly apposed to one another and also to a dendritic spine (sp), to which the lower of two TH varicosities is also juxtaposed. G and H illustrate in adjacent thin sections the very rare occurrence of a dually labeled terminal in the nAcb of adult rats neonatally lesioned with 6-OHDA. Scale bar = 0.5 μm .

TABLE 3. Mean Number of Immunoreactive Axon Terminals in the Nucleus Accumbens, Neostriatum, and Substantia Nigra of Normal Or 6-OHDA-Lesioned Immature (P15) and Mature (P90) Rats¹

| | TH | | VGLUT2 | | TH/VGLUT2 | |
|--------|---------------------|---------------------|-----------|-----------|---------------------------|-------|
| | P15 | P90 | P15 | P90 | P15 (%) | P90 |
| Normal | | | | | | |
| nAcb | 115 ± 6 | 64 ± 4 | 82 ± 21 | 97 ± 5 | 45 ± 5 (28) | 0 |
| NStr | 152 ± 12 | 109 ± 4 | 0.7 ± 0.4 | 0.3 ± 0.1 | 17 ± 6 (17) | 0 |
| 6-OHDA | | | | | | |
| nAcb | 63 ± 7 ³ | 15 ± 2 ³ | 46 ± 9 | 108 ± 13 | 37 ± 4 (37 ²) | 6/120 |
| SN | 29 ± 1 | 20 ± 3 | 44 ± 17 | 47 ± 3 | 22 ± 6 (46) | 0 |

¹An equivalent thin section surface of 1,665 μm^2 was examined in each region and each rat, as explained in Materials and Methods. Mean \pm SEM per rat, for the total number of rats and of axon terminals given in Tables 4-6. In parentheses, the number of dually labeled terminals (TH/VGLUT2) is expressed as a percentage of all terminals containing TH.

² $P < 0.05$ for 6-OHDA-lesioned vs. normal rats of the same age.

³ $P < 0.001$ for 6-OHDA-lesioned vs. normal rats of the same age.

TABLE 4. Structural Features of immunoreactive Axon Terminals in the Nucleus Accumbens of Normal or 6-OHDA-Lesioned Immature (P15) and Mature (P90) Rats¹

| | TH | | VGLUT2 | | TH/VGLUT2 |
|--------------------------------------|---------------------|-----------------------|-------------|----------------------------|--------------------------|
| | P15 | P90 | P15 | P90 | P15 |
| Normal | | | | | |
| Total number | 807 | 511 | 574 | 779 | 318 |
| Mean diameter (μm) | 0.49 ± 0.02 | 0.49 ± 0.02 | 0.54 ± 0.02 | 0.69 ± 0.02 ^{3,8} | 0.58 ± 0.04 ² |
| Percentage with synaptic junction | 14 ± 2 | 3 ± 1 ⁸ | 21 ± 2 | 36 ± 2 ⁸ | 34 ± 3 |
| Length of junction (μm) | 0.17 ± 0.02 | 0.19 ± 0.02 | 0.19 ± 0.02 | 0.28 ± 0.01 ⁷ | 0.16 ± 0.03 |
| Synaptic incidence (%) | 37 ± 5 | 7 ± 1 ⁸ | 58 ± 6 | 96 ± 6 ⁸ | 110 ± 9 |
| 6-OHDA-lesioned | | | | | |
| Total number | 440 | 120 | 325 | 860 | 256 |
| Mean diameter (μm) | 0.52 ± 0.03 | 0.53 ± 0.03 | 0.58 ± 0.03 | 0.70 ± 0.01 ^{3,7} | 0.64 ± 0.03 ² |
| Percentage with synaptic junction | 25 ± 2 ⁵ | 9 ± 2 ^{4,8} | 21 ± 2 | 37 ± 2 ⁸ | 34 ± 5 |
| Length of junction (μm) | 0.16 ± 0.01 | 0.22 ± 0.04 | 0.14 ± 0.01 | 0.26 ± 0.01 ⁸ | 0.13 ± 0.03 |
| Synaptic incidence (%) | 70 ± 6 ⁶ | 22 ± 5 ^{4,8} | 71 ± 8 | 106 ± 7 ⁷ | 130 ± 20 |

¹An equivalent thin section surface of 1,665 μm^2 was examined in each rat, as explained in Materials and Methods. Mean \pm SEM per rat, from seven rats at P15 and eight rats at P90, for the total number of terminals indicated. In view of their absence in normal rat and very small numbers after 6-OHDA lesion, no values are listed for TH/VGLUT2-immunopositive axon terminals in mature (P90) rats. See Results for description of differences between categories of labeled terminals at the same age.

² $P < 0.05$ vs. TH.

³ $P < 0.001$ vs. TH.

⁴ $P < 0.05$ between terminals in a given category in normal or 6-OHDA-lesioned rats of the same age.

⁵ $P < 0.01$ between terminals in a given category in normal or 6-OHDA-lesioned rats of the same age.

⁶ $P < 0.001$ between terminals in a given category in normal or 6-OHDA-lesioned rats of the same age.

⁷ $P < 0.01$ between terminals of a given category in normal or 6-OHDA-lesioned rats according to age.

⁸ $P < 0.001$ between terminals of a given category in normal or 6-OHDA-lesioned rats according to age.

the VGLUT2 terminals were significantly larger than the TH terminals ($P < 0.05$; Table 6). The synaptic incidence of terminals labeled for TH only was remarkably high at P15 (78%) and much lower at P90 (14%; $P < 0.01$). As in both nAcb and NStr, the terminals labeled for VGLUT2 only were not all synaptic at P15 (65%) as opposed to P90 (104%; $P < 0.05$). Again, the extrapolated synaptic incidence of the terminals dually labeled for TH/VGLUT2 at P15 was over 100% (120%), suggesting that many of these varicosities made more than a single synaptic contact. The synaptic incidence for all TH axon terminals at P15 was 97% and therefore much higher than at P90 ($P < 0.001$).

DISCUSSION

This study demonstrates a regression of the dual TH/VGLUT2 phenotype of mesencephalic DA neurons with age in three conditions: normal maturation (in nAcb and NStr), after its reactivation by a lesion (in VTA and nAcb), and during the growth of a neoinnervation (in SN). Moreover, in all three conditions, the presence of VGLUT2 protein in DA axon terminals appeared to be associated with the formation of synaptic junctions by these terminals, which suggests a particular role for glutamate in the establishment of synaptic junctions by mesencephalic DA neurons.

Methodological considerations

Even though there were no reasons to doubt the specificity of the immunocytochemical signals observed in the present study, it could not be ascertained that all TH and/or VGLUT2 axon terminals were actually identified under the conditions of these double-immunolabeling experiments. In tissue prepared for electron microscopy, the preembedding immunogold technique used to detect VGLUT2 is notoriously less sensitive than the immunoperoxidase-DAB technique, and the penetration of immunoreagents is limited. For these reasons, our quantitative evaluation of the number of axon terminals in the different categories of labeling was restricted to the superficial parts of embedded tissue sections, and the number of axon terminals in each categories of immunolabeling had to be considered as relative estimates rather than true numbers. Even more importantly, when axon terminals failed to show TH and/or VGLUT2 immunoreactivity, this did not mean that the corresponding proteins were absent, but could indicate merely that they were present in insufficient concentration to be detected.

Insofar as the electron microscopic examination was carried out in single thin sections, the number of varicosities in each category of immunolabeling was an approximation of their real number in the tissue, because larger varicosities had a greater

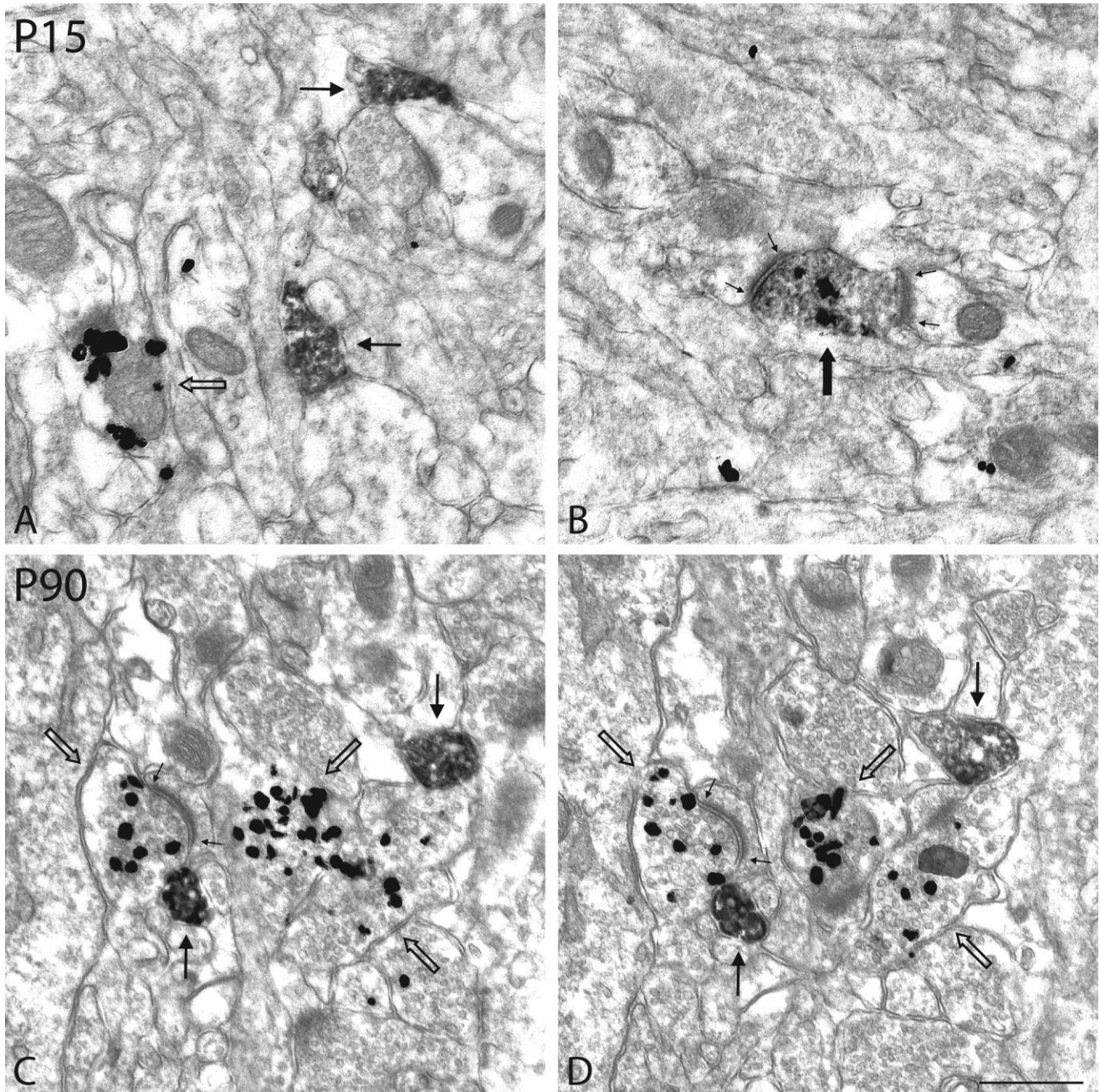


Figure 7. Immunoreactive axon terminals from the NStr of normal P15 (A,B) and P90 (C,D) rats after dual immunolabeling for TH (immunoperoxidase-DAB) and VGLUT2 (immunogold). In A, an axon terminal labeled for VGLUT2 (open arrow) and two smaller varicosities labeled for TH (thin arrows) are seen. In B, a dually labeled varicosity (thick arrow) forms two asymmetrical synaptic contacts (between small arrows) onto small dendritic profiles. C and D demonstrate in adjacent thin sections the presence of VGLUT2 and TH axon terminals close to one another. Note the asymmetrical synapse (between small arrows) formed by the VGLUT2 terminal on the left. Scale bar = 0.5 μ m.

chance of being detected than smaller ones. For this reason, the percentages of TH/VGLUT2 terminals over all TH terminals, as provided in Table 3, were recalculated after applying Abercrombie's formula to the counts (Abercrombie, 1946). This formula, $T/T + h$, where T = section thickness and h = the mean diameter of the objects, yields a ratio of "real" vs. observed number (Guillery, 2002), which was applied to the total number of vari-

cosities in each category. When recalculated for "corrected" numbers, the percentages of TH/VGLUT2 over all TH terminals did not markedly differ, amounting to 25% and 35% instead of 28% and 37% in the nAcb of normal and 6-OHDA-lesioned P15 rats, respectively; 15% instead of 17% in the NStr of normal P15 rats; and 37% instead of 46% in the SN of the 6-OHDA-lesioned P15 rats.

TABLE 5. Structural Features of Immunoreactive Axon Terminals in the Neostriatum of Immature (P15) and Mature (P90) Normal Rats¹

| | TH | | VGLUT2 | | TH/VGLUT2 |
|--------------------------------------|-----------------|-----------------|-----------------|-------------------|-------------------|
| | P15 | P90 | P15 | P90 | P15 |
| Total number | 242 | 345 | 174 | 205 | 52 |
| Mean diameter (μm) | 0.41 ± 0.01 | 0.43 ± 0.01 | 0.57 ± 0.07 | 0.60 ± 0.03^3 | 0.53 ± 0.03^2 |
| Percentage with synaptic junction | 9 ± 0.4 | 3 ± 1^5 | 26 ± 1^4 | 36 ± 4^3 | 38 ± 4^3 |
| Length of junction (μm) | 0.19 ± 0.01 | 0.16 ± 0.01 | 0.19 ± 0.02 | 0.22 ± 0.02 | 0.20 ± 0.01 |
| Synaptic incidence (%) | 18 ± 1 | 6 ± 2^5 | 70 ± 4^4 | 99 ± 12^3 | 93 ± 11^3 |

¹Means \pm SEM per rat from three rats at each age, for the total number of terminals indicated. No TH/VGLUT2-immunopositive axon terminals were observed in mature (P90) rats. See Results for description of differences between categories of labeled terminals at the same age.

² $P < 0.05$ vs. TH.

³ $P < 0.01$ vs. TH.

⁴ $P < 0.001$ vs. TH.

⁵ $P < 0.01$ between P15 and P90 normal rats.

Regression of the dual TH/VGLUT2 phenotype

In the three brain regions examined, there was an almost complete disappearance of TH-immunopositive axon terminals labeled for VGLUT2 between P15 and P90. This was in keeping with the marked reduction in number of neurons observed by double in situ hybridization to contain both TH and VGLUT2 mRNA in the VTA of P15 and P90 rats neonatally lesioned with 6-OHDA. The fact that such a decrease was not apparent in normal rats probably was due to the relative insensitivity of the double in situ hybridization technique, also evidenced by the difference in number of doubly labeled neurons visualized in the adult VTA with this technique (see also Yamaguchi et al., 2007) compared with a combination of TH immunocytochemistry and VGLUT2 in situ hybridization (Kawano et al., 2006) or with single-cell RT-PCR (Mendez et al., 2008). The difference between P15 and P90 would become apparent by double in situ hybridization when the amount of VGLUT2 mRNA would be increased in the DA neurons as a result of reactivation of the dual phenotype by the lesion (Dal Bo et al., 2008).

In view of its previous demonstration in the SN of postnatal rat (Janec and Burke, 1993; Oo and Burke, 1997), developmental cell death of DA neurons had to be considered as a possible explanation for the disappearance of axon terminals dually labeled for TH and VGLUT2 between P15 and P90. However, this naturally occurring phenomenon involves very few SN cells after P15, and it has not been demonstrated to occur in the VTA. It could therefore hardly account for the selective loss of the relatively large number of axon terminals that ceased to display both proteins, as observed in the nAcb and NStr of mature rat. Two other theoretical possibilities had to be considered: an elimination of only those axon terminals containing both proteins or, conversely, the addressing and progressive segregation of these proteins in different axonal branches of the same neurons. The former possibility was readily excluded, because it was clear from the light microscopic examination of TH-immunostained material that the density of TH labeling did not significantly decrease between P15 and P90 in any of the conditions or regions examined, including the SN after neonatal 6-OHDA lesion. As for the segregation hypothesis, already envisaged by Sulzer et al. (1998) and Dal Bo et al. (2004) on the basis of observations in tissue culture, it could not be formally excluded from our observations in nAcb or NStr. However, it was hardly compatible with our data on the size of terminals showing only TH vs. those showing only VGLUT2 or TH/VGLUT2 in the DA neoin-

ervation condition, unless we postulate that, by addressing TH and VGLUT2 to separate axonal branches, an equal number of doubly labeled varicosities would be converted into only TH and only VGLUT2 varicosities. Indeed, one would have then expected a change in the proportion of smaller vs. larger terminals between P15 and P90, which was not actually the case (43.0% at P15, 43.6% at P90).

Although this is speculative, a more likely explanation was an activation of the VGLUT2 gene in DA neurons during their growth, followed by a repression of its transcription in mature DA neurons. Several studies have already suggested that the dual phenotype of DA neurons is a transient phenomenon associated with growth, either during development (Dal Bo et al., 2008; Kawano et al., 2006; Yamaguchi et al., 2007) or in response to injury (Dal Bo et al., 2004; Mendez et al., 2008). In the present study, this would explain why the DA neoinnervation in substantia nigra, which develops only postnatally, is the region displaying the greatest proportion of TH terminals colocalizing VGLUT2 at P15. It would also account for the fact that, in P15 rats, a greater proportion of doubly labeled axon terminals was found in nAcb than in NStr, in which the maturation of the DA innervation appears to be more advanced than in nAcb at that age (Tarazi et al., 1998).

Ultrastructural characteristics

In the present study, particular attention was paid to the frequency with which the axon terminals (varicosities) in the various categories of immunolabeling made a synapse. Because the electron microscopic observations were made in single ultrathin sections, stereological extrapolation of the synaptic incidence for the whole volume of varicosities required a measurement of their average diameter and the length of visible junctions. In doing this, novel information was acquired on the intrinsic as well as relational features of DA terminals during normal development, following 6-OHDA lesion, and after aberrant sprouting and also of glutamatergic terminals during normal development.

In all conditions and regions examined, including SN, the axon terminals labeled for TH were comparable in size and appearance at P15 and P90, even though the aberrant fibers in SN were still growing at P15, as evidenced by their much greater number at P90 than at P15 (Fig. 2; see also Fernandes Xavier et al., 1994). Thus, varicosities belonging to growing DA fibers look mature and should be capable of transmitter release, including those doubly labeled for TH and VGLUT2. Another characteristic of the terminals labeled for TH was the

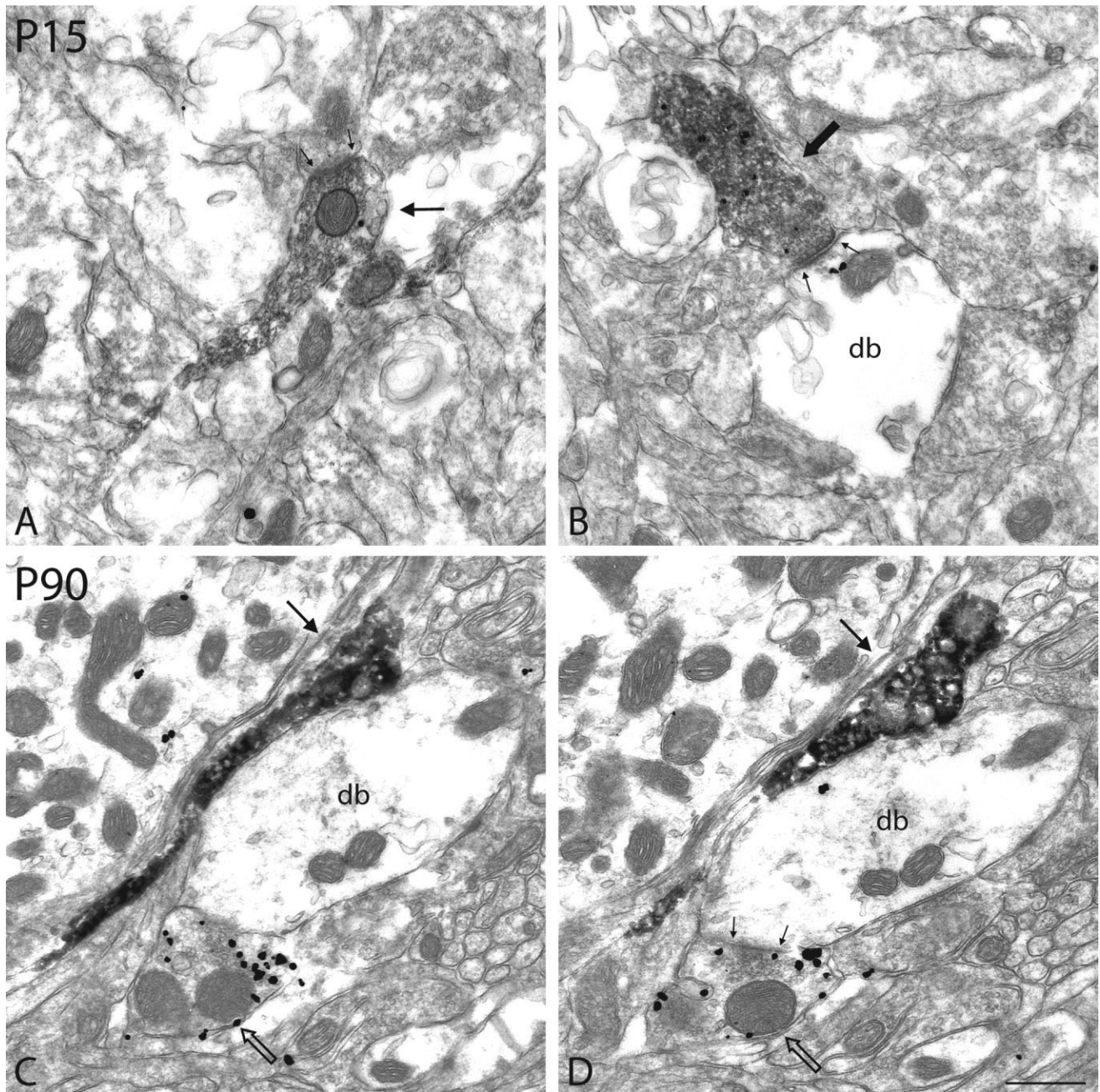


Figure 8.

Immunoreactive axon terminals of the DA neoinnervation in SN of 6-OHDA-lesioned P15 (A,B) and P90 (C,D) rats, after dual immunolabeling for TH (immunoperoxidase-DAB) and VGLUT2 (immunogold). In A, the singly labeled TH terminals (thin arrow) appear to be synaptic (between small arrows), as was often the case for these varicosities at P15. B is an example (thick arrow) of the many dually labeled varicosities that were then found to be all synaptic (between small arrows) in the remnants of SN. This synaptic junction is made onto a large dendritic branch (db). C and D illustrate in adjacent thin sections the presence of TH (thin arrows) as well as VGLUT2 axon varicosities (open arrows) in the remnants of SN, at an age when its DA neoinnervation no longer displays doubly labeled varicosities. In D, note the small synaptic contact (between arrows) made by the VGLUT2 varicosity with the large dendritic branch (db) to which the TH varicosity is also juxtaposed. Scale bar = 0.5 μm .

relatively high frequency with which they made synapse at P15 compared with adult. This difference was already significant in the nAcb and NStr of normal rat but was even greater in the case of the residual TH terminals of the nAcb after 6-OHDA lesioning and of the neoinnervation in SN. A similar

trend for higher synaptic incidence of DA varicosities during postnatal development had already been observed by Antonomopoulos et al. (2002), who reported that DA-immunoreactive axon terminals from the dorsal and ventral striatum of P14 rats were much more frequently synaptic than at P21.

TABLE 6. Structural Features of Immunoreactive Axon Terminals in the Substantia Nigra of Immature (P15) and Mature (P90) 6-OHDA-Lesioned Rats¹

| | TH | | VGLUT2 | | TH/VGLUT2 |
|--------------------------------------|-----------------|-----------------|-----------------|-------------------|-----------------|
| | P15 | P90 | P15 | P90 | P15 |
| Total number | 86 | 61 | 133 | 140 | 67 |
| Mean diameter (μm) | 0.50 ± 0.06 | 0.50 ± 0.04 | 0.64 ± 0.04 | 0.75 ± 0.06^2 | 0.73 ± 0.09 |
| Percentage with synaptic junction | 34 ± 4 | 5 ± 1^6 | 25 ± 4 | 34 ± 1^3 | 39 ± 3 |
| Length of junction (μm) | 0.23 ± 0.02 | 0.17 ± 0.03 | 0.26 ± 0.02 | 0.25 ± 0.01^6 | 0.24 ± 0.01 |
| Synaptic incidence (%) | 78 ± 9 | 14 ± 3^6 | 65 ± 11 | $104 \pm 2^{3,5}$ | 120 ± 10^4 |

¹Means \pm SEM from three rats at each age, for the total number of terminals indicated. No TH/VGLUT2 immunopositive terminals were observed in mature (P90) rats. See Results for description of differences between categories of labeled terminals at the same age.

² $P < 0.05$ vs. TH.

³ $P < 0.001$ vs. TH.

⁴ $P < 0.05$ vs. TH and VGLUT2.

⁵ $P < 0.05$ between P15 and P90 6-OHDA-lesioned rats.

⁶ $P < 0.01$ and between P15 and P90 6-OHDA-lesioned rats.

Our values for the nAcb and NStr of normal P15 rat were much lower than those in that particular study, presumably because of differences in sampling and also an underestimation of the synaptic frequency in our heavily labeled TH material, in which dense DAB precipitate on the plasmalemma of immunopositive profiles could obscure the presence of small, symmetrical synaptic junctions, as expected for these terminals (see, e.g., Descarries et al., 1996; Moss and Bolam, 2008). This was much less likely to occur in the case of the TH/VGLUT2 terminals, which always appeared to be less densely TH immunostained and displayed prominent and relatively large synaptic junctions, much as the terminals labeled for VGLUT2 only. A similar explanation probably accounted for the 7% and 6% values of synaptic incidence for TH-immunoreactive terminals in adult rat nAcb and NStr, which were considerably lower than previously found after radioautographic labeling of neostriatal DA terminals by [³H]DA uptake radioautography or DA immunocytochemistry (Descarries et al., 1996). As for the relatively high synaptic incidences of TH terminals measured here at both P15 and P90 in the nAcb and SN of neonatally 6-OHDA-lesioned rats, they were in keeping with the fact that many of these terminals were presumably those of growing axons, thus recapitulating the frequent synaptic relationships observed during normal development.

In contrast to the TH only terminals, the terminals labeled for VGLUT2 only appeared to be morphologically immature in the nAcb at P15; they were significantly smaller and displayed shorter synaptic junctions at P15 than at P90 in both normal and 6-OHDA-lesioned rats. This immaturity was also indicated by the fact that these VGLUT2 terminals were not yet all synaptic, as they would become in the adult (present study; see also Fujiyama et al., 2006; Lacey et al., 2005; Moss and Bolam, 2008). In this context, it was all the more striking to find that all dually labeled TH/VGLUT2 terminals at P15, whether in the normal nAcb or NStr or in the nAcb and the neoinnervation of SN after 6-OHDA lesioning, did make a synaptic junction. This suggested a link between the presence of VGLUT2 and the formation of synapses by these terminals.

Role of VGLUT2 in growing DA neurons

It is likely that glutamate can be released by axonal boutons that contain one of its vesicular transporters. Both in culture (Bourque and Trudeau, 2000; Joyce and Rayport, 2000; Sulzer

et al., 1998) and suggested in vivo (Chuhma et al., 2004; Lavin et al., 2005), strong physiological evidence has accumulated for the release of glutamate by axon terminals of mesencephalic DA neurons. Glutamate released from DA axon terminals could be implicated in developmental events such as proliferation, migration, differentiation, and arbor size development (for review see Cline and Haas, 2008; Ruediger and Bolz, 2007). It could also act as a signal for the establishment of synaptic junctions by growing axons, as recently proposed on the basis of in vivo observations on the pausing of synaptic vesicle protein transport vesicles at predefined sites along growing axons (Sabo et al., 2006). Moreover, during postnatal development or in response to injury, the presence of VGLUT2 in DA terminals could allow for a greater intravesicular accumulation and release of DA than at maturity, as recently demonstrated to be the case for VGLUT3 and acetylcholine in striatal cholinergic interneurons of adult rat (Gras et al., 2008). Whether the regression of the dual glutamatergic phenotype would then have something to do with the loss of junctions by mature DA terminals is an intriguing possibility. In this regard, it would be of interest to determine whether the localization of VGLUT2 is more frequent or persistent in DA axon terminals of the anteromedial or the occipital cortex that appear to be mostly if not entirely synaptic in the adult, contrary to those in dorsal and ventral striatum.

ACKNOWLEDGMENTS

N.B.-C. was the recipient of a studentship from the GRSNC and FRISQ. The plasmids used to prepare VGLUT2 probe were kindly provided by Dr. S. El Mestikawy. The authors thank Jérôme Maheux for his help with the in situ hybridization experiments.

LITERATURE CITED

- Abercrombie M. 1946. Estimation of nuclear population from microtome sections. *Anat Rec* 94:239–247.
- Antonopoulos J, Dori I, Dinopoulos A, Chiotelli M, Parnavelas JG. 2002. Postnatal development of the dopaminergic system of the striatum in the rat. *Neuroscience* 110:245–256.
- Bai L, Xu H, Collins JF, Ghishan FK. 2001. Molecular and functional analysis of a novel neuronal vesicular glutamate transporter. *J Biol Chem* 276:36764–36769.
- Beaudet A, Sotelo C. 1981. Synaptic remodeling of serotonin axon terminals in rat agranular cerebellum. *Brain Res* 206:305–329.
- Boulland JL, Qureshi T, Seal RP, Rafiki A, Gundersen V, Bergersen LH, Fremeau RT Jr, Edwards RH, Storm-Mathisen J, Chaudhry FA. 2004.

- Expression of the vesicular glutamate transporters during development indicates the widespread corelease of multiple neurotransmitters. *J Comp Neurol* 480:264–280.
- Bourque MJ, Trudeau LE. 2000. GDNF enhances the synaptic efficacy of dopaminergic neurons in culture. *Eur J Neurosci* 12:3172–3180.
- Chuhma N, Zhang H, Masson J, Zhuang X, Sulzer D, Hen R, Rayport S. 2004. Dopamine neurons mediate a fast excitatory signal via their glutamatergic synapses. *J Neurosci* 24:972–981.
- Cline H, Haas K. 2008. The regulation of dendritic arbor development and plasticity by glutamatergic synaptic input: a review of the synaptotrophic hypothesis. *J Physiol* 586:1509–1517.
- Cossette M, Parent A, Lévesque D. 2004. Tyrosine hydroxylase-positive neurons intrinsic to the human striatum express the transcription factor Nurr1. *Eur J Neurosci* 20:2089–2095.
- Dal Bo G, St.-Gelais F, Danik M, Williams S, Cotton M, Trudeau LE. 2004. Dopamine neurons in culture express VGLUT2 explaining their capacity to release glutamate at synapses in addition to dopamine. *J Neurochem* 88:1398–1405.
- Dal Bo G, Bérubé-Carrière N, Mendez JA, Leo D, Riad M, Descarries L, Lévesque D, Trudeau LE. 2008. Enhanced glutamatergic phenotype of mesencephalic dopamine neurons after neonatal 6-hydroxydopamine lesion. *Neuroscience* 156:59–70.
- Descarries L, Watkins KC, Garcia S, Bosler O, Doucet G. 1996. Dual character, asynaptic and synaptic, of the dopamine innervation in adult rat neostriatum: a quantitative autoradiographic and immunocytochemical analysis. *J Comp Neurol* 375:167–186.
- Descarries L, Bérubé-Carrière N, Riad M, Dal Bo G, Mendez JA, Trudeau LE. 2008. Glutamate in dopamine neurons: synaptic vs. diffuse transmission. *Brain Res Rev* 58:290–302.
- Fernandes Xavier FG, Doucet G, Geffard M, Descarries L. 1994. Dopamine reinnervation in the substantia nigra and hyperinnervation in the interpeduncular nucleus of adult rat following neonatal cerebroventricular administration of 6-hydroxydopamine. *Neuroscience* 59:77–87.
- Freneau RT Jr, Troyer MD, Pahner I, Nygaard GO, Tran CH, Reimer RJ, Bellocchio EE, Fortin D, Storm-Mathisen J, Edwards RH. 2001. The expression of vesicular glutamate transporters defines two classes of excitatory synapse. *Neuron* 31:247–260.
- Freneau RT Jr, Voglmaier S, Seal RP, Edwards RH. 2004. VGLUTs define subsets of excitatory neurons and suggest novel roles for glutamate. *Trends Neurosci* 27:98–103.
- Fujiyama F, Unzai T, Nakamura K, Nomura S, Kaneko T. 2006. Difference in organization of corticostriatal and thalamostriatal synapses between patch and matrix compartments of rat neostriatum. *Eur J Neurosci* 24:2813–2824.
- Gras C, Herzog E, Belenchi GC, Bernard V, Ravassard P, Pohl M, Gasnier B, Giros B, El Mestikawy S. 2002. A third vesicular glutamate transporter expressed by cholinergic and serotonergic neurons. *J Neurosci* 22:5442–5451.
- Gras C, Amilhon B, Lepicard EM, Poirel O, Vinatier J, Herbin M, Dumas S, Tzavara ET, Wade MR, Nomikos GG, Hanoun N, Saurini F, Kemel ML, Gasnier B, Giros B, El Mestikawy S. 2008. The vesicular glutamate transporter VGLUT3 synergizes striatal acetylcholine tone. *Nat Neurosci* 11:292–300.
- Gratto KA, Verge VM. 2003. Neurotrophin-3 down-regulates trkA mRNA, NGF high-affinity binding sites, and associated phenotype in adult DRG neurons. *Eur J Neurosci* 18:1535–1548.
- Guillery RW. 2002. On counting and counting errors. *J Comp Neurol* 447:1–7.
- Hanaway J, McConnell JA, Netsky MG. 1971. Histogenesis of the substantia nigra, ventral tegmental area of Tsai and interpeduncular nucleus: an autoradiographic study of the mesencephalon in the rat. *J Comp Neurol* 142:59–73.
- Harkany T, Hartig W, Berghuis P, Dobszay MB, Zilberter Y, Edwards RH, Mackie K, Ernors P. 2003. Complementary distribution of type 1 cannabinoid receptors and vesicular glutamate transporter 3 in basal forebrain suggests input-specific retrograde signalling by cholinergic neurons. *Eur J Neurosci* 18:1979–1992.
- Haycock JW. 1993. Multiple forms of tyrosine hydroxylase in human neuroblastoma cells: quantitation with isoform-specific antibodies. *J Neurochem* 60:493–502.
- Herzog E, Belenchi GC, Gras C, Bernard V, Ravassard P, Bedet C, Gasnier B, Giros B, El Mestikawy S. 2001. The existence of a second vesicular glutamate transporter specifies subpopulations of glutamatergic neurons. *J Neurosci* 21:RC181.
- Hökfelt T, Mårtensson R, Björklund A, Kleinau S, Goldstein M. 1984. Distributional maps of tyrosine-hydroxylase-immunoreactive neurons in the rat brain. In: Björklund A, Hökfelt T, editors. *Handbook of chemical neuroanatomy*, vol 2. Amsterdam: Elsevier. p 277–379.
- Jackson D, Bruno JP, Stachowiak MK, Zigmond MJ. 1988. Inhibition of striatal acetylcholine release by serotonin and dopamine after the intracerebral administration of 6-hydroxydopamine to neonatal rats. *Brain Res* 457:267–273.
- Janec E, Burke RE. 1993. Naturally occurring cell death during postnatal development of the substantia nigra pars compacta of rat. *Mol Cell Neurosci* 4:30–35.
- Joyce MP, Rayport S. 2000. Mesoaccumbens dopamine neuron synapses reconstructed in vitro are glutamatergic. *Neuroscience* 99:445–456.
- Kawano M, Kawasaki A, Sakata-Haga H, Fukui Y, Kawano H, Nogami H, Hisano S. 2006. Particular subpopulations of midbrain and hypothalamic dopamine neurons express vesicular glutamate transporter 2 in the rat brain. *J Comp Neurol* 498:581–592.
- Lacey CJ, Boyes J, Gerlach O, Chen L, Magill PJ, Bolam JP. 2005. GABA_B receptors at glutamatergic synapses in the rat striatum. *Neuroscience* 136:1083–1095.
- Lavin A, Nogueira L, Lapish CC, Wightman RM, Phillips PE, Seamans JK. 2005. Mesocortical dopamine neurons operate in distinct temporal domains using multimodal signaling. *J Neurosci* 25:5013–5023.
- Liguz-Leczna M, Skangiel-Kramska J. 2007. Vesicular glutamate transporters (VGLUTs): the three musketeers of glutamatergic system. *Acta Neurobiol Exp* 67:207–218.
- Mendez JA, Bourque MJ, Dal Bo G, Bourdeau ML, Danik M, Williams S, Lacaille JC, Trudeau LE. 2008. Developmental and target-dependent regulation of vesicular glutamate transporter expression by dopamine neurons. *J Neurosci* 28:6309–6318.
- Moss J, Bolam JP. 2008. A dopaminergic axon lattice in the striatum and its relationship with cortical and thalamic terminals. *J Neurosci* 28:11221–11230.
- Ni B, Rostock PR Jr, Nadi NS, Paul SM. 1994. Cloning and expression of a cDNA encoding a brain-specific Na⁺-dependent inorganic phosphate cotransporter. *Proc Natl Acad Sci U S A* 91:5607–5611.
- Ni B, Wu X, Yan GM, Wang J, Paul SM. 1995. Regional expression and cellular localization of the Na⁺-dependent inorganic phosphate cotransporter of rat brain. *J Neurosci* 15:5789–5799.
- Oo TF, Burke RE. 1997. The time course of developmental cell death in phenotypically defined dopaminergic neurons of the substantia nigra. *Brain Res Dev Brain Res* 98:191–196.
- Paxinos G, Watson C. 2005. *The rat brain in stereotaxic coordinates*. New York: Elsevier Academic Press.
- Persson S, Boulland JL, Aspling M, Larsson M, Freneau RT Jr, Edwards RH, Storm-Mathisen J, Chaudhry FA, Broman J. 2006. Distribution of vesicular glutamate transporters 1 and 2 in the rat spinal cord, with a note on the spinocervical tract. *J Comp Neurol* 497:683–701.
- Peters A, Palay SL. 1996. *The morphology of synapses*. *J Neurocytol* 25:687–700.
- Riad M, Garcia S, Watkins KC, Jodoïn N, Doucet E, Langlois X, El Mestikawy S, Hamon M, Descarries L. 2000. Somatodendritic localization of 5-HT1A and preterminal axonal localization of 5-HT1B serotonin receptors in adult rat brain. *J Comp Neurol* 417:181–194.
- Ruediger T, Bolz J. 2007. Neurotransmitters and the development of neuronal circuits. *Adv Exp Med Biol* 621:104–115.
- Sabo SL, Gomes RA, McAllister AK. 2006. Formation of presynaptic terminals at predefined sites along axons. *J Neurosci* 26:10813–10825.
- Schafer MK, Varoqui H, Defamie N, Weihe E, Erickson JD. 2002. Molecular cloning and functional identification of mouse vesicular glutamate transporter 3 and its expression in subsets of novel excitatory neurons. *J Biol Chem* 277:50734–50748.
- Stachowiak MK, Bruno JP, Snyder AM, Stricker EM, Zigmond MJ. 1984. Apparent sprouting of striatal serotonergic terminals after dopamine-depleting brain lesions in neonatal rats. *Brain Res* 291:164–167.
- Stornetta RL, Sevigny CP, Schreihof AM, Rosin DL, Guyenet PG. 2002. Vesicular glutamate transporter DNPI/VGLUT2 is expressed by both C1 adrenergic and nonaminergic presympathetic vasomotor neurons of the rat medulla. *J Comp Neurol* 444:207–220.
- Sulzer D, Joyce MP, Lin L, Geldwert D, Haber SN, Hattori T, Rayport S. 1998. Dopamine neurons make glutamatergic synapses in vitro. *J Neurosci* 18:4588–4602.
- Takamori S, Rhee JS, Rosenmund C, Jahn R. 2001. Identification of differentiation-associated brain-specific phosphate transporter as a

- second vesicular glutamate transporter (VGLUT2). *J Neurosci* 21:RC182.
- Takamori S, Malherbe P, Broger C, Jahn R. 2002. Molecular cloning and functional characterization of human vesicular glutamate transporter 3. *EMBO Rep* 3:798–803.
- Tarazi FI, Tomasini EC, Baldessarini RJ. 1998. Postnatal development of dopamine and serotonin transporters in rat caudate-putamen and nucleus accumbens septi. *Neurosci Lett* 254:21–24.
- Trudeau LE. 2004. Glutamate co-transmission as an emerging concept in monoamine neuron function. *J Psychiatry Neurosci* 29:296–310.
- Umbriaco D, Watkins KC, Descarries L, Cozzari C, Hartman BK. 1994. Ultrastructural and morphometric features of the acetylcholine innervation in adult rat parietal cortex: an electron microscopic study in serial sections. *J Comp Neurol* 348:351–373.
- Voorn P, Kalsbeek A, Jorritsma-Byham B, Groenewegen HJ. 1988. The pre- and postnatal development of the dopaminergic cell groups in the ventral mesencephalon and the dopaminergic innervation of the striatum of the rat. *Neuroscience* 25:857–887.
- Yamaguchi T, Sheen W, Morales M. 2007. Glutamatergic neurons are present in the rat ventral tegmental area. *Eur J Neurosci* 25:106–118.
- Zhou J, Nannapaneni N, Shore S. 2007. Vesicular glutamate transporters 1 and 2 are differentially associated with auditory nerve and spinal trigeminal inputs to the cochlear nucleus. *J Comp Neurol* 500:777–787.